

BEARING CAPACITY OF OPEN-ENDED PILES IN SAND

by

Arif Kıvanç Yılmaz

B.S., in C.E., Yıldız Technical University, 2004

Submitted to the Institute for Graduate Studies in  
Science and Engineering in partial fulfillment of  
the requirements for the degree of  
Master of Science

Graduate Program in Civil Engineering

Boğaziçi University

2007

## **ACKNOWLEDGEMENTS**

I would like to express my sincere gratitude to my thesis supervisor, Professor Erol Güler, for his continuous support, guidance and encouragement through the preparation of this thesis.

I would also like to thank Assistant Professor Mehmet Berilgen for his valuable suggestions and patience during the preparation of this dissertation.

I am thankful to all of the members of my family, and I would like to dedicate this thesis to my grandmother.

## ABSTRACT

### BEARING CAPACITY OF OPEN-ENDED PILES IN SAND

The aim of this study is to evaluate the loading capacity of open ended piles in cohesionless soils by using PLAXIS. The simulation program PLAXIS uses finite element method to calculate load capacity and solve the problem. At the beginning of the study, the model for simulation was rough and less detailed. In the advancing steps, the model was changed and improved according to test results to be more realistic and correct.

Axisymmetric model was used for this simulation. In the model, the parameters at pile surrounding and especially the pile toe were changed to understand the effect to pile capacity. Internal friction angle, modulus of elasticity, active lateral pressure  $K_0$  and the interval of  $K_{02}$  change rates were the selected parameters. At the end of the tests, the effect and the magnitude of the effects due to parameter changes were examined.

A 15 meter open ended pile was modeled and the entire tests were conducted on the same type of pile to compare results easily. To model extra squeezing and probable “plugging” condition at the inner part of the pile, a special zone in this inner part with higher E values was created. One of the aims was to understand the contribution of this “plugging” zone to load capacity. After modeling was completed, the factor of safety values under various loads was calculated. To derive the ultimate load capacity under varying parameters, piles were loaded until collapsing will occur.

Test results show that, the most effective parameter for load capacity in this kind of problem is the characteristics of soil at the pile toe and pile toe neighborhood. The increments or change of soil parameters in the inner side of the pile do not produce a remarkable effect on load capacity. That small changes in results may caused by the solution method of PLAXIS (Finite Element Method). Because the non-breaking and non-tearing finite triangular elements of PLAXIS, producing a flawless simulation model is hard to apply.

## ÖZET

### AÇIK UÇLU KAZIKLARIN KUMLU ZEMİNLERDEKİ TAŞIMA KAPASİTESİ

Bu çalışma kohezyonsuz zeminlerde açık uçlu kazıkların taşıma kapasitelerinin sonlu elemanlar metodu kullanan PLAXIS adlı program vasıtası ile hesaplanmasını amaçlamaktadır. Önceleri kaba bir modelden ibaret olan simülasyon, çalışmanın ilerleyen safhalarında modeli gerçeğe ve kusursuza daha yakın hale getirmek amacıyla test sonuçları uyarınca değiştirilmiş, geliştirilmiştir.

Aksisimetrik modelde, kazık çevresi ve özellikle uç bölgesinde zemin parametreleri ile oynanarak farklı koşullar altında değişkenlerin nasıl sonuçlar doğurduğu incelenmiştir. Burada amaç hangi parametrelerin taşıma gücüne etkisi olup olmadığı ve eğer varsa ne kadar etkili olduğunu anlamaktır.

Sonuçlar arasında rahatça kıyaslama yapabilmek için aynı özelliklere sahip 15 metrelik açık uçlu çelik kazık modellenmiş, kazık içinde kalan zeminin sıkışması durumunu - ve dolayısıyla muhtemel “tıkanma” vakasını - modelleyebilmek içinse, kazık içinde çevresindeki zemine nazaran daha rijit zemin parametrelerine sahip özel bir bölge oluşturulmuştur. Amaçlardan birisi de bu sıkışan ve “kemerlenen” bölgenin taşıma gücünü arttırıp arttırmadığını ve - eğer varsa - taşıma gücüne ne kadar katkısının bulunduğunu araştırmaktır. Model tamamlandıktan sonra, öncelikle muhtelif yükler altındaki açık uçlu kazığın güvenlik katsayıları hesaplatılmış, akabinde nihai taşıma gücünü anlamak amacıyla sistem göçene kadar yük artımı yapılmıştır.

Deney sonuçları taşıma gücünü etkileyen en önemli parametrelerin, kazığın uç bölgesinin çevresindeki zeminin parametreleri olduğunu göstermiştir. Kazık içinde kalan bölgedeki zemin parametrelerinin değişiminin taşıma gücüne dikkat çekici bir katkısı olamamaktadır. Burada sonuçlarda büyük bir değişiklik olmamasının bir sebebi de PLAXIS’ in sonlu elemanlar metodu kullanmasındadır. Zira yükleme uyarınca koparılamayan veya parçalanamayan PLAXIS’ in sonlu üçgen elemanları gerçekçi bir modelleme yapmayı kısmen de olsa engellemektedir.

## TABLE OF CONTENTS

ACKNOWLEDGEMENTS .....	iii
ABSTRACT.....	iv
ÖZET .....	v
LIST OF FIGURES .....	viii
LIST OF TABLES.....	xi
LIST OF SYMBOLS/ABBREVIATIONS.....	xii
1. INTRODUCTION .....	1
2. PILE TYPES.....	3
2.1 Overview of Typical Pile Types .....	3
2.2 Pile Types Due to Their Bearing Properties .....	4
2.2.1 End-Bearing Piles .....	4
2.2.2. Friction Piles.....	4
2.2.3. Composite Piles .....	4
2.3. Pile Types Due to Their Method of Construction.....	5
2.3.1 Displacement Piles.....	5
2.3.1.1. Driven Piles.....	5
2.3.1.2. Driven and Cast in Place Piles .....	5
2.3.1.3. Bored Piles .....	5
2.4. Classification Due to Material Properties of Piles.....	6
2.4.1. Timber Piles.....	6
2.4.2 Concrete Piles .....	7
2.4.2.1. Precast Concrete Piles.....	7
2.4.2.2. Cast-in-Place Concrete Piles.....	11
2.4.3. Steel Piles.....	16
2.4.3.1. Steel H-Piles.....	16
2.4.3.2. Steel Pipe Piles.....	17
3. BEARING CAPACITY OF PILES .....	18
3.1. Condition Change in Soils Due to Pile Existence.....	19
3.1.1. Piles in Cohesionless Soils .....	19
3.1.2. Piles in Cohesive Soils.....	20

3.2. Load Transfer in Piles.....	21
4. INTRODUCTION TO PLAXIS .....	23
4.1. General Modelling Aspects .....	27
4.1.1. Components of Mesh.....	27
5. SIMULATION OF MODEL .....	29
5.1. Mesh Generation.....	29
5.2. Manual Calculation of Bearing Capacity.....	38
6. RESULTS .....	42
6.1. Factor of Safety Values.....	42
7. CONCLUSIONS.....	46
APPENDIX A.....	47
REFERENCES .....	58

## LIST OF FIGURES

Figure 2.1. General pile classification chart .....	3
Figure 2.2. Typical pre-stressed concrete piles .....	9
Figure 2.3. Typical details of conventionally reinforced concrete piles .....	10
Figure 2.4. Concrete cylinder pile .....	11
Figure 3.1. Compaction of cohesionless soils during driving of piles .....	19
Figure 3.2. Disturbance of cohesive soils during driving of piles .....	21
Figure 3.3. Typical load transfer profiles .....	22
Figure 4.1. Stress points and nodes for a finite triangle element.....	28
Figure 5.1. Coarse mesh .....	30
Figure 5.2. Medium mesh.....	31
Figure 5.3. Very fine mesh .....	31
Figure 5.4. Ring load (a) and Pile cross section (b) .....	33
Figure 5.5. Distance of influence for piles and chosen “ $K_0$ intervals” .....	33
Figure 5.6. Negligible loads preventing tension cracks.....	34
Figure 5.7. Extended interface and varying $K_0$ 's.....	35
Figure 5.8. Deformation with a weighted soil .....	36

Figure 5.9. Deformation when a “weightless” soil is used.....	36
Figure 5.10. Complete simulation model .....	37
Figure 5.11. Pile problem .....	38
Figure 5.12. Bearing capacity factor $N_q^*$ in granular soils .....	39
Figure 6.1. Settlements with different mesh coarsenesses .....	42
Figure 6.2. Varying stiffness values at right side of the pile .....	44
Figure A.1. Factor of safety with 100 kN ring load, $\varphi=31^0$ , $R_{interface}= 0.5$ .....	47
Figure A.2. Factor of safety with 200 kN ring load, $\varphi=31^0$ , $R_{interface}= 0.5$ .....	47
Figure A.3. Factor of safety with 300 kN ring load, $\varphi=31^0$ , $R_{interface}= 0.5$ .....	48
Figure A.4. Factor of safety with 100 kN ring load, $\varphi=33^0$ , $R_{interface}= 0.5$ .....	48
Figure A.5. Factor of safety with 200 kN ring load, $\varphi=33^0$ , $R_{interface}= 0.5$ .....	49
Figure A.6. Factor of safety with 300 kN ring load, $\varphi=33^0$ , $R_{interface}= 0.5$ .....	49
Figure A.7. Factor of safety with 400 kN ring load, $\varphi=33^0$ , $R_{interface}= 0.5$ .....	50
Figure A.8. Factor of safety with 100 kN ring load, $\varphi=35^0$ , $R_{interface}= 0.5$ .....	50
Figure A.9. Factor of safety with 200 kN ring load, $\varphi=35^0$ , $R_{interface}= 0.5$ .....	51
Figure A.10. Factor of safety with 300 kN ring load, $\varphi=35^0$ , $R_{interface}= 0.5$ .....	51

Figure A.11. Factor of safety with 400 kN ring load, $\varphi=35^0$ , $R_{\text{interface}}=0.5$ .....	52
Figure A.12. Factor of safety with 100 kN ring load, $\varphi=31^0$ , $R_{\text{interface}}=0.75$ .....	52
Figure A.13. Factor of safety with 200 kN ring load, $\varphi=31^0$ , $R_{\text{interface}}=0.75$ .....	53
Figure A.14. Factor of safety with 300 kN ring load, $\varphi=31^0$ , $R_{\text{interface}}=0.75$ .....	53
Figure A.15. Factor of safety with 100 kN ring load, $\varphi=33^0$ , $R_{\text{interface}}=0.75$ .....	54
Figure A.16. Factor of safety with 200 kN ring load, $\varphi=33^0$ , $R_{\text{interface}}=0.75$ .....	54
Figure A.17. Factor of safety with 300 kN ring load, $\varphi=33^0$ , $R_{\text{interface}}=0.75$ .....	55
Figure A.18. Factor of safety with 400 kN ring load, $\varphi=33^0$ , $R_{\text{interface}}=0.75$ .....	55
Figure A.19. Factor of safety with 100 kN ring load, $\varphi=35^0$ , $R_{\text{interface}}=0.75$ .....	56
Figure A.20. Factor of safety with 200 kN ring load, $\varphi=35^0$ , $R_{\text{interface}}=0.75$ .....	56
Figure A.21. Factor of safety with 300 kN ring load, $\varphi=35^0$ , $R_{\text{interface}}=0.75$ .....	57
Figure A.22. Factor of safety with 400 kN ring load, $\varphi=35^0$ , $R_{\text{interface}}=0.75$ .....	57

**LIST OF TABLES**

Table 2.1.	Categories of timber piles .....	6
Table 5.1.	Global coarseness levels .....	29
Table 5.2.	Soil properties .....	38
Table 5.3.	Static load capacities due to the factor of safety values.....	41
Table 6.1.	Factor of safety values with different Young's Moduluses.....	43
Table 6.2.	Factor of safety values with different interface coefficients.....	43
Table 6.3.	Ultimate load capacities of piles under different soil parameters .....	45

## LIST OF SYMBOLS / ABBREVIATIONS

$A$	Pile area
$A_p$	Pile area
$A_s$	Shaft surface area
$A_t$	Pile toe area
$b$	Pile diameter
$c$	Cohesion
$d$	Outer diameter of steel pipe pile
$d_1$	Inner diameter of steel pipe pile
$D$	Diameter of pile
$E$	Young's Modulus
$E_{ref}$	Young's Modulus in PLAXIS
$f_s$	Unit shaft resistance
$f_{ult}$	Ultimate stress
$I$	Moment of inertia
$k_x$	Permeability among x direction
$k_y$	Permeability among y direction
$l_e$	Average element size
$n_c$	Mesh distinction coefficient in PLAXIS
$N_q^*$	Bearing capacity factor
$q$	Effective vertical stress
$q_t$	Unit toe resistance
$Q_a$	Allowable load
$Q_p$	Toe bearing capacity of pile
$Q_s$	Shaft bearing capacity of pile
$Q_u$	Axial ultimate load

$R_{interface}$	Interface coefficient in PLAXIS
$R_s$	Shaft resistance
$R_t$	Toe resistance
$s$	Settlement
$u$	Pore water pressure
$x_{min}$	Outer geometry dimension for mesh element
$x_{max}$	Outer geometry dimension for mesh element
$y_{min}$	Outer geometry dimension for mesh element
$y_{max}$	Outer geometry dimension for mesh element
$\gamma_{dry}$	Unit weight above phreatic line
$\gamma_{wet}$	Unit weight below phreatic line
$\Sigma Msf$	Total factor of safety
$\tau$	Shear stress
$\phi$	Internal friction angle

## 1. INTRODUCTION

Piles are the construction elements used to support or transfer the superstructure loads to the ground. They are long and slender in design and can be consist of different material types. Timber, steel and concrete materials can be used for pile manufacturing. Load can be transferred to the layers which are deeper than the ground surface or directly supported by the pile itself. This “directly supporting” states three ways: End bearing, shaft bearing or both.

Use of piles is more expensive than shallow foundation solutions but under some circumstances pile using is a requirement for structure security. They can be used when the upper layers in the ground are not suitable and secure enough to bear the superstructure loads. In this condition, piles can carry the loads and transfer them to a more reliable, “high-level load capacity” soil. If the layer is so deep that the project is becoming non-feasible, shaft bearing can be projected for the pile. Piles can also be used for compensating the lateral loads in high-rise structures caused by wind or earthquake loads. Another application area of the piles is transferring the loads from “active zone” which can swell or suddenly collapse when interact with water.

Piles can resist the forces on the raft foundations under groundwater or sea platforms, which are exposed to lifting force of water. Also they can be used to prevent the effects of erosion in sour region for piers. The displacement piles may stiffen loose granular soils. By this way the load capacity of soil can be increased.

It is important that a pile foundation be installed to meet the design requirements for compressive, lateral and uplift capacity. This may dictate driving piles for a required ultimate capacity or to a predetermined length established by the designer. It is equally important to avoid pile damage or foundation cost overruns by excessive driving. These objectives can all be satisfactorily achieved by use of wave equation analysis, dynamic monitoring of pile driving, and static load testing.

Construction of a successful driven pile foundation that meets the design objectives depend on relating the requirements of the static analysis methods presented on the plans to the dynamic methods of field installation and construction control. The tools for obtaining such a foundation must be explicitly incorporated into the plans and specifications as well as included in the contract administration of the project.

Knowledgeable construction supervision and inspection are the keys to proper installation of piles. State-of-the-art designs and detailed plans and specifications must be coupled with good construction supervision to achieve desired results.

Post construction review of pile driving results versus predictions regarding pile driving resistances, pile length, field problems, and load test capacities is essential. These reviews add to the experience of all engineers involved on the project and will enhance their skills.

Calculation for static load capacity of a pile can be done by both manually or using a computer program. Because of the numerous parameters (Young's modulus for different kinds of soils, internal friction angles, interface factors, varying lateral earth pressures) in problem, manual calculation is not feasible and applicable. Due to these limitations PLAXIS, a program which uses finite element equations for solution, is used. The solution is prepared by modeling whole simulation with finite triangular elements. These elements can not be separated or disintegrated. Since the triangular finite elements can not be disintegrated, the model is not flawless to simulate a rupturing soil.

## 2. PILE TYPES

### 2.1. Overview of Typical Pile Types

Piles can be classified due to their bearing properties, type of construction they used for or their material properties, but they can be widely categorized in two main types: foundation piles for support of structural loads and sheet piles for earth retention systems.

Foundation piles can be classified on the basis of their method of load transfer from the pile to the surrounding soil mass. The transfer of load can be by shaft resistance, end bearing resistance or a combination of both. Figure 2.1. shows general pile classification.

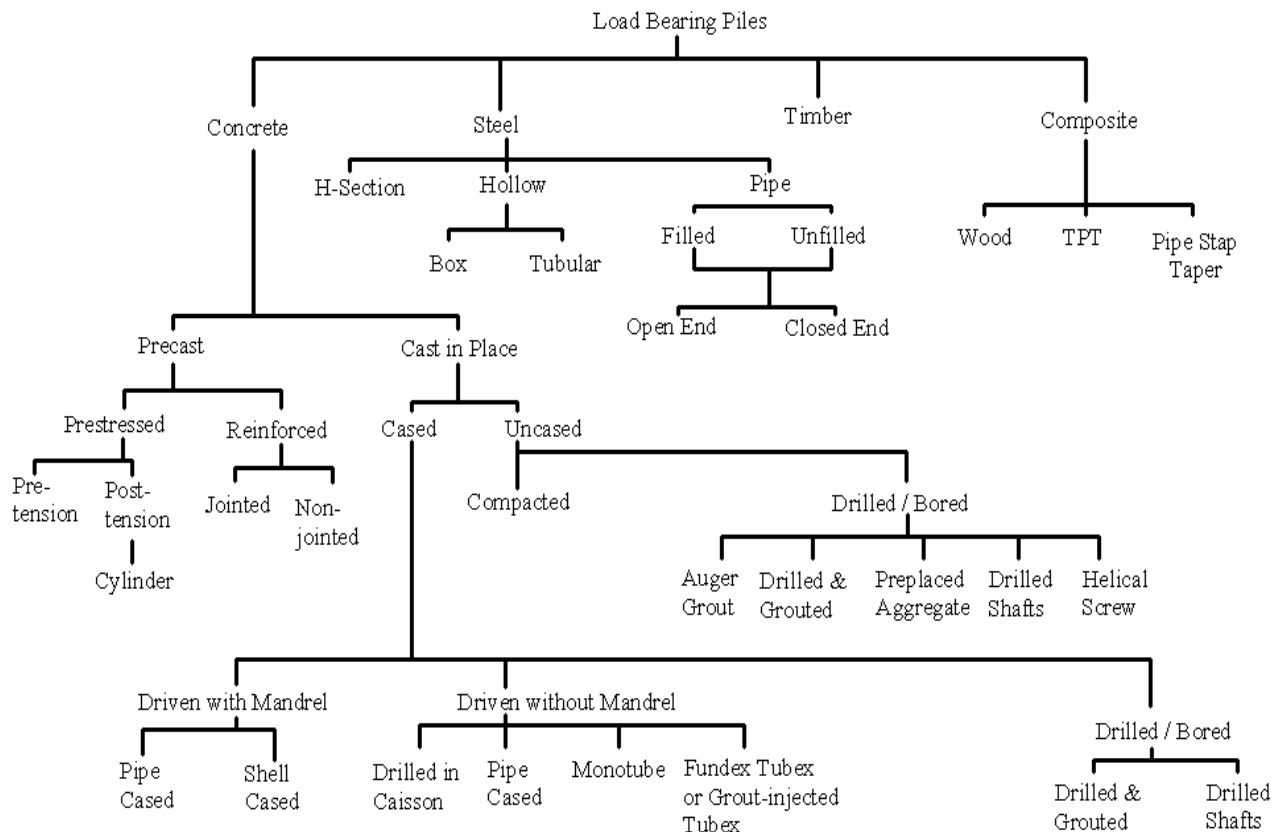


Figure 2.1. General pile classification chart

## **2.2. Pile Types Due to Their Bearing Properties**

### **2.2.1. End-Bearing Piles**

This kind of piles practically derives all their support from the rock or soil near the toe point, and very little amount from surrounding the upper part (shaft). When calculating the capacity of an end-bearing pile, the important point is deriving the properties of the material at the toe of the pile. The ultimate bearing capacity of the pile increases with increasing bearing area. And it is obvious that the capacity of piles with large toe diameters is greater than piles with small point diameters.

### **2.2.2 Friction Piles**

Friction piles derive their support mostly from the surrounding soil through the developed shearing resistance between the soil and the pile. Due to end-bearing piles, load carried by the soil near the toe of the pile has very small percentage. Capacity of the pile depends on the characteristics of the surrounding material.

### **2.2.3. Composite Piles**

The Composite piles are produced by using different materials as the name implies. It could be advantageous to use composite piles for areas of hazardous ground water but the cost and the application difficulty of forming a suitable joint makes this kind of piles less preferable.

## 2.3. Pile Types Due to Their Method of Construction

### 2.3.1. Displacement Piles

In the use of displacement piles, the soil is shifted during the pile driving or jacking into the ground. There are different types of displacement piles

2.3.1.1. Driven Piles. These kinds of piles are driven to the soil by the blows of a hammer. The description of the pile driving equipment will be given later briefly. Driven piles are not damaged by ground heave. Since they can be manufactured in long lengths, they give a very big advantage to geotechnical engineers. But with the increasing diameters of driven piles the risk of breaking during hard driving increases. This undesired situation can cause replacement charges and delays on construction site.

2.3.1.2. Driven and Cast-in-Place Piles. Driven and Cast-in-place piles are made built by driving a tube with a closed end into the soil, and filling the tube with concrete. After the driving the tube may or may not be withdrawn. If the tube is driven with a closed end, it excludes ground water. The types of the driven and cast-in-place piles are: cased driven shell concrete piles and uncased concrete piles. Both cased and uncased piles have subgroups.

2.3.1.3. Bored Piles. In this method, firstly the soil is removed by boring a hole into which concrete is placed or different types of precast concrete or other units are inserted. Bored piles can be installed in very large diameters and very long lengths. Ground heave does not occur during in this piling method. But the boring may loosen sandy and gravelly soils, and may cause waisting or necking in soil.

## 2.4. Classification Due to Material Properties of Piles

### 2.4.1. Timber Piles

Timber piles are usually produced round, tapered cross section made from tree trunks driven the small end down. Pine, fir and oak could be used for piles.

Timber piles are best suited for modest loads when used as friction piles in sands, silts and clays. Especially in loose sands, the taper of timber piles is effective in increasing the shaft resistance. Timber piles are appropriate for the construction of bridge fender systems and small jetties due to the good energy absorption properties of wood. But they are not recommended in soils such as dense gravel, boulders, till or for toe bearing piles on rock since they are vulnerable to damage at the pile head and toe in hard driving. Fibers of timber piles can crush or the pile may broom at the pile head due to overdriving. To prevent this undesirable situation, a helmet with cushion material or metal strapping around the head of the pile can be used. Under hard driving conditions, a metal shoe should be attached to the pile toe.

There are limitations of timber piles on the size of the tip and butt end as well as the misalignment can be tolerated. The Chicago Building Code requires that the tip have minimum diameter of 150 mm. and the butt 250 mm. if the pile is less than 7.6 m. And have a 100 mm. butt if the pile is more than 7.6 m. Long. The standard of alignment is that a straight line from the center of the butt to the center of the tip lies within the pile shaft.

Table 2.1. : Categories of timber piles, ASCE Manual 17 (Bowles, 1988)

Class	Min. Diameter
Class A : Used for heavy loads and / or large unsupported lengths	360mm
Class B: Used for medium loads	300 mm
Class C: Use below the permanent water table or for temporary works	300mm

When the timber piles are used under the ground water table, their durability is considered as limitless. But when a timber pile is subjected to alternate wetting/drying cycles or located above the water table, damage and decay by insects may occur. Wood preservatives such as Chromated Copper Arsenate (CCA) and Ammoniacal Copper Zinc Arsenate (ACZA) should be used to prevent the damages that reduce the service life of the timber pile.

The durability of a timber pile in various conditions is:

1. Foundation piles submerged in ground water will last indefinitely.
2. Fully embedded, treated foundation piles partially above the ground water with a concrete cap will last 100 years or longer.
3. Treated piles in fresh water will last about five to ten years less than land trestle piles in the same area.
4. The longevity of the treated piles in brackish water should be determined by the experience in the area.

#### **2.4.2. Concrete Piles**

Concrete piles may be precast and cast in place construction.

2.4.2.1. Precast Concrete Piles. This general classification covers both conventionally reinforced concrete and pre-stressed concrete piles. Piles in this category are formed in a central casting yard to the specified length, cured, and then shipped to the construction site. If space is available and sufficient quantities of piles are needed, casting yard may be provided at the site to reduce transportation costs. Generally concrete piles are cast with a hollow core. The hollow core may be used for a jet pipe, for placing instrumentation during construction, or for determining pile damage. Usually precast concrete piles are manufactured in constant cross section, but can also include a tapered section near the pile toe. Precast piles may be made using ordinary reinforcement. These are designed for bending stresses during pickup and transport to the site, for bending moments from lateral

loads, and to provide sufficient resistance to the vertical loads and any tension forces developed during driving.

This type of piles may be used as friction piles when driven in sand, gravel, or clays. When using in boulder conditions, a short piece of structural H-section may be cast into or attached to the pile toe for penetrating through the zone of cobbles and boulders. A rock shoe or 'Oslo point' cast into the pile toe can assist seating of concrete piles into a rock surface. Precast concrete piles are capable of high capacities when used as toe bearing piles.

Precast concrete piles are considered resistant to corrosion but can be damaged by direct chemical attack, electrolytic action or oxidation. Concrete can be protected from chemical attack by use of special cements and coatings.

- Pre-stressed Concrete Piles

Pre-stressed concrete piles consist of a configuration similar to a conventional reinforced concrete pile except that the longitudinal reinforcing steel is replaced by the pre-stressing steel. This type of piles are formed by tensioning high strength steel ( $f_{ult}$  of 1705 to 1860 MPa) pre-stressing cables to some value on the order of 0.5 to 0.7  $f_{ult}$  and casting the concrete pile about the cable. When the concrete hardens, the pre-stress cables are cut. With the tension force in the cables, a compressive stress is produced.

Sections of the pre-stressed concrete piles vary from the most common solid square to a solid octagonal section. These piles are used especially for friction piles in sands, gravels and clays where a known pile length is required since pre-stressed piles can be difficult to shorten.

Pre-stressed piles can be pre-tensioned or post-tensioned. Pre-tensioned piles are usually cast to their full length in permanent casting beds. Post-tensioned piles are usually manufactured in sections and assembled and pre-stressed to the required pile lengths at the manufacturing plant or the yard. Comparing to the conventional reinforced concrete piles, pre-stressed piles are more durable. Since the concrete is under continuous compression, hairline cracks are kept tightly closed and thus pre-stressed piles are usually more resistant

to weathering and corrosion than conventionally reinforced piles. Because of this particularity of pre-stressed piles corrosion is not as a serious problem as for reinforced concrete. Also the tensile stresses that can develop in the concrete under certain driving and handling conditions are less critical for pre-stressed concrete piles. But these types of piles are more vulnerable to damage from striking hard layers of soil or obstructions during driving than reinforced concrete piles. This risk occurs because of the decrease in axial compression capacity which results from the application of the pre-stressing force. Figure 2.2. shows the typical pre-stressed concrete piles.

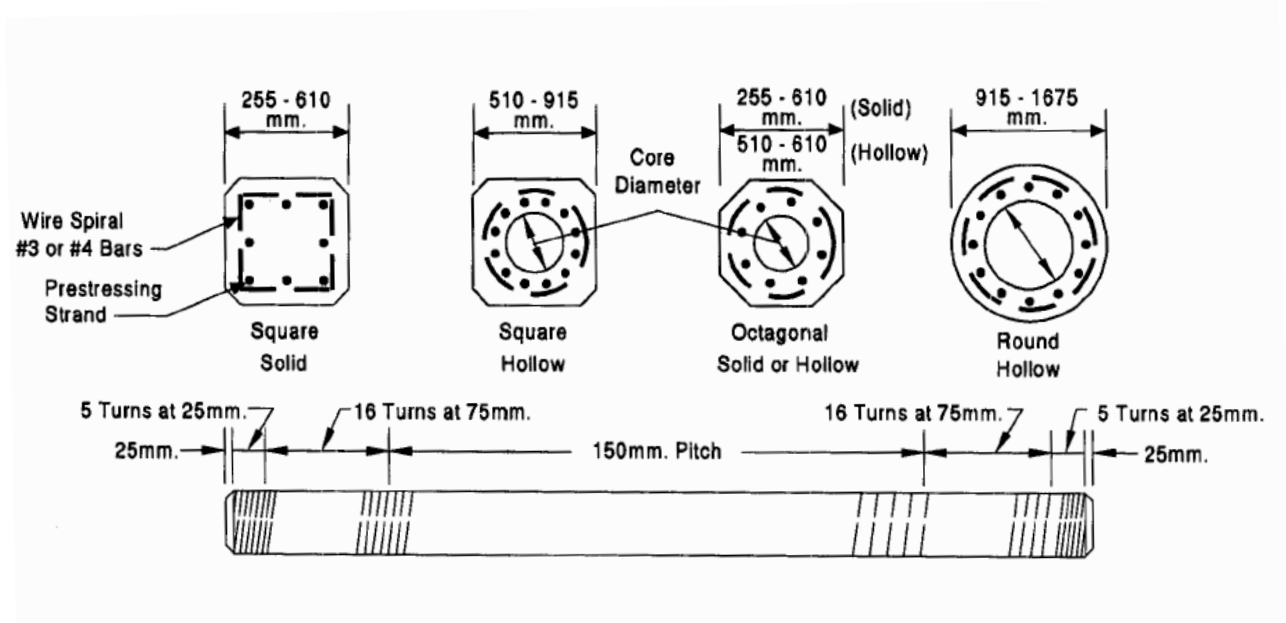


Figure 2.2. Typical pre-stressed concrete piles (after PCI, 1993)

- Reinforced Concrete Piles

Reinforced concrete piles are manufactured from concrete and have reinforcement which consist of a steel cage made up of several longitudinal bars and lateral or tie steel in the form of individual hoops or a spiral. Due to pre-stressed piles, reinforced concrete piles are more susceptible to damage during handling and driving because of tensile stresses. The risk of pile head cracking is lower than pre-stressed concrete piles. Additionally reinforced concrete piles are easier to splice than pre-stressed piles and thus may be used when variable pile lengths are needed. However splices should be located below the ground surface to prevent corrosion, or if under water below the mud line.

Reinforced concrete piles are used infrequently in the United States. However, in Europe, Australia, and many Asian countries reinforced piles are used routinely based on economic considerations. The figure below shows the typical details of conventionally reinforced concrete piles.

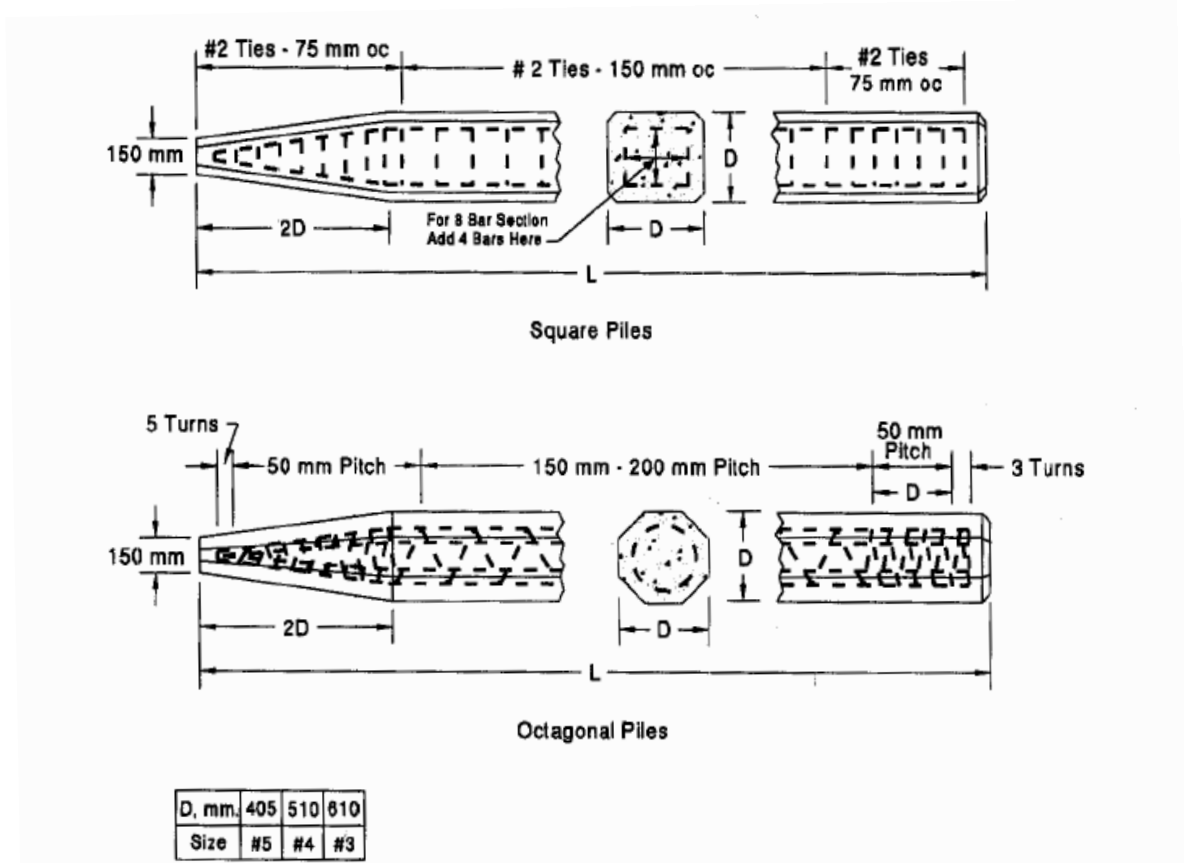


Figure 2.3. Typical Details of Conventionally Reinforced Concrete Piles (after PCA, 1951)

- Concrete Cylinder Piles

A concrete cylinder pile is post-tensioned, hollow concrete pile which is cast in sections, bonded with a plastic joint compound, and then post tensioned in lengths containing several segments. The piles typically extend above ground and are designed to resist a combination of axial loads and bending moments. The range of pile diameter is from 915 to 1675 mm. Special type of concrete is cast by a process unique to cylinder pile which achieve high density and low porosity.

Concrete cylinder piles are generally used for marine structures or land trestles due to their high resistance to corrosion. They are sometimes considerably difficult to drive. However, they usually extend directly to the superstructure support level avoiding the need for a pile cap, which can result in substantial cost savings.

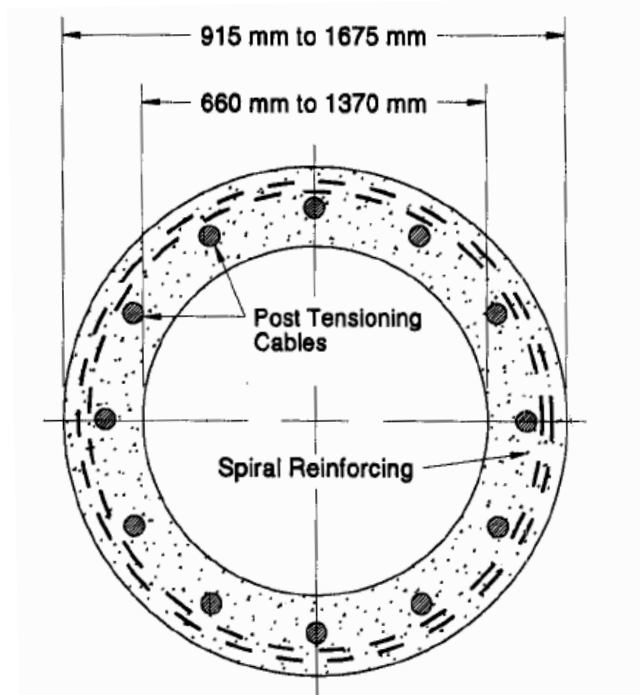


Figure 2.4. Concrete cylinder pile (Design and Construction of Driven Pile Foundations, U.S. Department of Transportation, 1998)

#### 2.4.2.2. Cast in Place Concrete Piles

These types of piles are installed by placing concrete in a steel shell that has been driven or inserted into a bored hole in the ground. The steel shell or casing may be left in place or withdrawn after the concrete is placed. Concrete is also placed in predrilled holes that are uncased. The casing may be driven with a mandrel, after which withdrawal of the mandrel empties the casing. A mandrel is usually a heavy tubular steel section inserted into the pile that greatly improves the pile drivability. The casing may also be driven with a driving tip on the point, providing a shell that is ready for filling with concrete immediately, or the casing may be driven open-end, the soil entrapped in the casing being jetted out after the driving is completed.

- Cased Driven Shell Concrete Piles

The cased driven shell concrete pile is the most widely used type of cast in place concrete pile. There are two principal types of cased piles. First type is driven without a mandrel and the other is driven with a mandrel. Shells driven without mandrels have thicknesses in the range of 3 to 63 mm. Shells driven with mandrels are much thinner, often 10 to 24 gages or 3.3 to 0.5 mm thick. The mandrel driven shells are usually crumpled circumferentially. That leads to excellent frictional characteristics and increased collapse strength prior to concrete placement. After driving, a shell pile is inspected internally along its full length before concrete is placed. When the concrete in pile may be under tension from such conditions as uplift, high lateral loads, or for unsupported pile lengths reinforcing steel is required.

a) Mandrel Driven Shell Concrete Piles

Mandrel driven shells can be used in most soil conditions except where obstacles such as cobbles and boulders are present that could damage the thin shells during driving. These types of thin shells are susceptible to collapse under hydrostatic pressure due to concrete placement. Mandrel driven shells are best suited for friction piles in granular material.

b) Monotube – Cased Concrete Piles

The Monotube pile is a proprietary pile driven without a mandrel. Monotubes are longitudinally fluted and they are tapered over the lower pile length. This fluted and tapered design of Monotube piles has several functional advantages:

- The flutes add stiffness which is necessary for handling and driving lightweight piles.
- The flutes increase the surface area while the tapered section improves the capacity per unit length in compression loading.

- The flutes are formed by the cold working which increases the yield point of the steel to more than 350 Mpa.

c) Pipe – Cased Concrete Piles

Pipe – cased can be driven either open or closed end. Closed end piles can be driven conventionally from the pile head, can be bottom driven with a mandrel, or by a mandrel engaged at both the pile head and toe. Open ended driven piles may require internal clean out if the pile will be concrete filled to some distance below grade.

d) Fundex Tubex or Grout-Injected Tubes Piles

The Fundex pile is a unique form of a pipe-cased, cast in place concrete pile. In the construction method the pile is screwed into the ground with a special iron drill point which is welded to the end of the first section of pipe. A drill table then forces the pile into the ground utilizing a constant vertical load and torque. When the first pipe section reaches a depth providing sufficient headroom for the attachment of a second pipe section, the second section is welded to the first and drilling continues. The pipe casing can be installed grouted or non-grouted due to soil conditions.

Some of the advantages of the Fundex Tubex piles include vibrationless and quiet installation, drilling equipment that can be used in confined spaces and a removable mast that allows installation with only 6 meters of overhead clearance.

e) Driven and Drilled-In Caisson Piles

The Drilled-In Caisson is a special type of high capacity, cased, cast in place pile used for large engineering structures. The casing of this pile is usually a heavy-walled pipe fitted with a drive shoe which is driven to bedrock and sealed off within the rock. When the casing reaches bedrock, it is cleaned out and a socket is drilled into the rock with rotary drilling equipment. Next the rock socket is cleaned, and a steel H-shaped core or reinforcing cage is placed before filling the rock socket and cased pipe with concrete.

- Uncased Concrete Piles

Two principal types of uncased piles exist which are bored piles and compacted concrete piles.

- a. Bored Piles

These types of piles are installed by drilling or augering a hole in the ground and filling it with concrete. Bored piles are susceptible to problems such as necking (smaller pile diameter at some locations along their length), grout contamination by soil, or borehole collapse. Bored, uncased piles have a high degree of risk for structural integrity.

There are several types of bored piles:

(1) Continuous flight auger (CFA) or auger – cast piles are usually installed by turning a continuous-flight hollow-stem auger into the ground to the required depth. As the auger is withdrawn, grout or concrete is pumped under pressure through the hollow stem, filling the hole from the bottom up. Frequently vertical reinforcing steel is pushed down into the grout or concrete shaft before it hardens. Uplift tension reinforcing can be installed by placing a single high strength steel bar through the hollow stem of the auger before grouting. After reinforcing steel is placed, the pile head is cleaned of any lumps of soil which may have fallen from the auger. Then the pile head is formed with a temporary steel sleeve to protect the fresh grout from contamination, or it is formed to the ground surface above the cutoff grade and later trimmed off to the cutoff elevation.

(2) Drilled shafts are installed by mechanically drilling a hole to the required depth and filling the hole with concrete. Sometimes an enlarged base is formed mechanically to increase the toe bearing area. Drilling slurry or a temporary liner can be used when the sides of the hole are unstable. Reinforcing steel is installed as a cage inserted prior to concrete placement. Drilled shafts are often used where large toe bearing capacities can be achieved, such as on rock or in glacial tills. They are also used where support is primarily

developed through shaft resistance in granular and cohesive soils, and rock. Drilled shafts are sometimes designed with a permanent steel casing.

(3) Drilled and grouted piles (micro piles) are installed by rotating a casing with a cutting edge into the soil or by percussion methods. Soil cuttings are removed with circulating drilling fluid. Reinforcing steel is then inserted and a sand-cement grout is pumped through a tremie. The bored hole is filled from the bottom up while casing is withdrawn. These piles are principally used for underpinning work, seismic retrofitting and landslide stabilization. Several types of micro piles leave the casing in place for added bending resistance and axial capacity.

(4) Pre-placed aggregate piles are installed by drilling a hole to the required depth, filling the hole with coarse aggregate, pumping grout into the column of aggregate, and filling it from the bottom top.

(5) Helical Screwcast in place piles are formed using the Atlas Piling System. The helical piles are displacement piles formed using a single-start auger head with a short flight. The auger head is carried on a hollow stem which transmits a large torque and compressive force as it is screwed into the ground to the required depth. After reinforcement is placed, concrete is poured through to the end of the hollow auger and the auger is slowly unscrewed and removed. This process leaves behind a screw-threaded cast in place pile with large threads which provide increased surface area for improved shaft resistance. In fact, for a given pile size and volume of concrete, pile capacities are greater than for traditionally constructed bored piles. The disadvantage of this pile type is that the restricted diameter of the reinforcement cage limits the bending capacity.

#### b. Compacted Concrete Piles

This type of pile is installed by bottom driving a temporary steel casing into the ground using a drop weight on a zero slump concrete plug at the bottom of the casing. After the required depth has been reached, the steel casing is restrained from above and the concrete plug is driven out the bottom of the tube. By adding and driving out small batches

of zero slump concrete an enlarged base is formed. These piles are best suited for loose to medium dense granular soils.

### **2.4.3. Steel Piles**

2.4.3.1. Steel H-Piles. These members are usually consisting of rolled wide flange sections that have flange widths approximately equal the section depth. Wide-flange beams or I beams may also be used; however, the H shape is especially proportioned to withstand the hard driving stress which the pile may be subjected. In these types of piles the flanges and web are of equal thickness. Steel H-piles are manufactured in standard sizes ranging from 200 to 360 mm. The standard WF and I shapes generally have a thinner web than flange.

Steel H-piles are used as toe bearing piles, and a combination of both shaft resistance and toe bearing piles. The steel H-pile is a small volume displacement pile due to small cross-section area. Because of this property steel H-piles can be driven more easily through dense granular layers and very stiff clays than displacement piles. In some cases H-piles may plug. When the soil being penetrated will adhere to the web and the inside flange surfaces create a closed-end, plugging occurs. The H-pile will tend to behave like a displacement pile below the depth of plug formation. The soil below the plug formation depth may remold, and this can have a strong effect on driving resistance and load capacity.

H piles have an advantage of sufficient rigidity that they will break smaller boulders or displace them to one side. However when big obstructions are encountered they have a tendency to deviate. These piles are also easily adjustable in length by welding or by bolting. Splices are commonly made by full penetration groove welds so that the splice is as strong as the pile in both compression and bending.

Because of the lack of oxygen in the soil, corrosion is not a practical problem for steel H-piles. But for the piles under the ground water table or piles that driven into fill materials protection for corrosion may be needed. One common protection method is the application of pile coatings before and after driving. Coal-tar epoxies, fusion bonded epoxies, metallized zinc, metallized aluminum and phenolic mastics may be used.

Selecting a bigger area for the cross-section of pile, and ignoring the loss of steel due to corrosion is another option for design. Also for the piles above ground water table, precast concrete jackets, encasement by cast in place concrete or cathodic protection may be applied.

2.4.3.2. Steel Pipe Piles. Pipe piles are welded or seamless steel pipes which may be driven either open-end or closed-end. They are often filled with concrete after driving, although in some cases this is not necessary. Steel pipe piles are manufactured in diameters ranging from 200 to 1220 mm. Their typical wall thicknesses range from 3 to 25mm (upper limit is to 64 mm but not preferred).

Pipe piles are used as a friction, toe bearing pile or for both. Due to convenience in splicing, these piles are used where variable pile lengths are required. They can be used in seismic areas with the increased ductility requirements for earthquake resistant design. Open-end piles have the advantage of surface entry to break up boulders encountered by either use of a chopping bit or blasting, drilling and removal of the rock pieces.

When the capacity from the full pile toe is needed, the pile is driven closed-end. A closed end pipe pile is generally formed by welding a 12 to 25 mm thick flat steel plate or a conical point to the pile toe. For driving processes into weathered rock or through boulders, a cruciform end plate or a conical point with rounded nose is generally used to prevent the distortion of pile toe. Open ended piles can be socketed into bedrock. During driving through dense materials open ended piles may form a soil plug like the steel H-piles mentioned above. The plug may significantly increase the pile toe resistance. The plug should not be removed unless the pile is to be filled with concrete. The pipe piles are spliced using full penetration groove welds.

### 3. BEARING CAPACITY OF PILES

Bearing capacity of piles can be calculated by static and dynamic analysis methods. Dynamic analysis methods can be defined as analytical techniques for evaluating the soil resistance against which the pile is driven. Static analysis methods can be categorized as analytical methods that use soil strength and compressibility properties to determine pile capacity and performance. Static analysis methods are an integral part of the design process and they are necessary to determine the most cost effective pile type and to estimate the number and design length of piles. Static analysis methods are relatively easy to apply due to dynamic analysis methods and beneficial to create a primary perspective for the construction design.

Static capacity of a pile is defined as the sum of soil resistance along the pile shaft and the resistance at the pile toe. The ultimate capacity of an individual pile and of a pile group is smaller of: the capacity of surrounding soil/rock medium to support the loads transferred from the piles or, the structural capacity of the pile(s). Static analysis calculations of the deformation response to lateral loads and of pile group settlement are compared to the performance criteria established for .

Static pile capacity can be derived by using SPT data, In-situ test data and laboratory determined shear strength parameters of the soil and rock surrounding the pile. The piles always influence the soil which is to be driven, because the foundation is almost always disturbed. Several factors affect the degree of disturbance. These include the soil type and density, the pile type (displacement, non-displacement), and the method of pile installation (driven, drilled, jetted). When a driven pile is installed, the remolding and substantial soil disturbance is inevitable. Two states exist: “During” and “After” pile driving. There are two conditions which are for cohesive and cohesionless soil.

### 3.1. Condition Change in Soils Due to Pile Existence

#### 3.1.1. Piles in Cohesionless Soils

The capacity of driven piles in cohesionless soils depends primarily on the relative density of the soil. During the driving process, the relative density of loose to medium dense cohesionless soil is increased close to the pile due to vibrations and lateral displacement of soil. This condition occurs especially in vicinity of displacement piles. Broms (1996) and more recent studies found the zone of densification extends as far as 3 to 5.5 diameters away from the pile shaft and 3 to 5 diameters below the pile toe as depicted in Figure 3.1. Increment in relative density is a preferable situation because the capacity of pile is also increased with relative density. The piles with large displacement characteristics (closed-end, precast concrete piles) increase the relative density of cohesionless material more than low displacement piles.

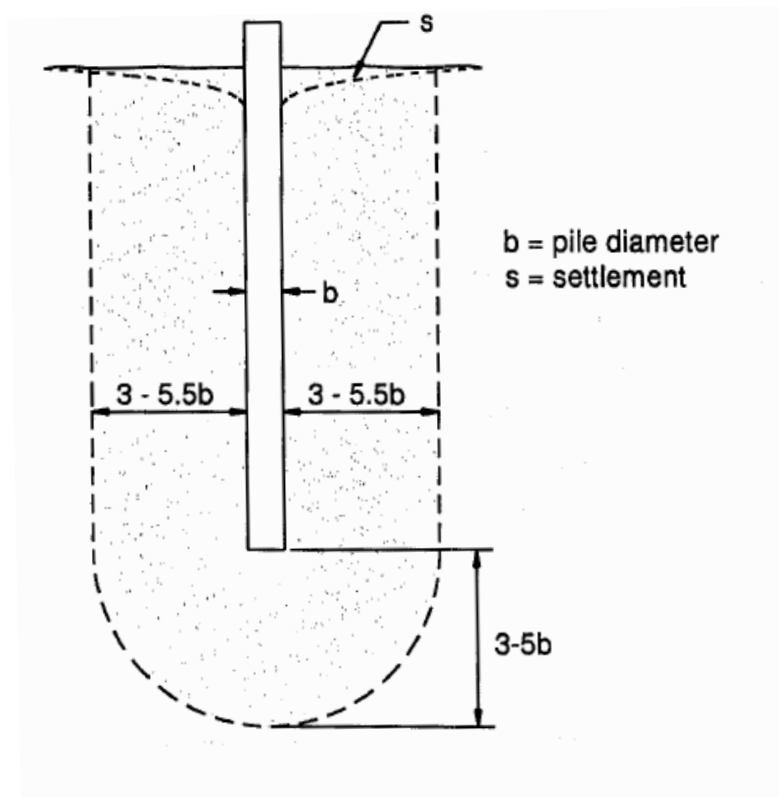


Figure 3.1. Compaction of cohesionless soils during driving of piles (Broms, 1966)

Due to relaxation in dense sand and gravels in time, the increase in horizontal ground stress that occurs adjacent to the pile during the driving process can be lost. The effective stress-shear stress equation can explain the phenomena:

$$\tau = c + (\sigma - u) \tan \phi \quad (3.1)$$

This situation occurs if the negative pore pressures generated during driving are diminish. The negative pore pressure occurs because of volume change and dilation of dense sand. Negative pore pressures temporarily increase the soil strength, and therefore pile capacity, by changing the  $(\sigma - u) \tan \phi$  component of shear strength to  $(\sigma + u) \tan \phi$ . With the decreasing negative pore pressures, both the shear strength and pile capacity decrease. When the process occurs in saturated cohesionless silts and loose to medium dense fine sands, high positive water pressures are generated. This positive pore pressures temporarily reduce the soil shear strength and the pile capacity which is same as the below described situation for cohesive soils. Increment in load capacity with time or soil set-up is mostly quicker for sands and silts than for clays because the pore pressures dissipate more rapidly in cohesionless soils due to cohesive soils.

### 3.1.2. Piles in Cohesive Soils

Due to the driving of piles into saturated cohesive materials, the soil near the piles is disturbed and radially compressed. In soft or normally consolidated clays, the zone of disturbance is generally within one pile diameter around the pile. When the piles are driven into saturated stiff clays, there are also significant changes in secondary soil structure (closing of fissures) with remolding and loss of previous stress history effects in the immediate vicinity of pile. Figure 3.2. shows the disturbance zone for piles driven in cohesive soils as observed by Broms (1966). The ground heave in cohesive soils caused by the displacement pile is also shown in Figure 3.2. below.

When the pile is driven, the disturbance and radial compression generate high positive pore pressures which temporarily reduce soil shear strength, and consequently the load capacity of pile. Whilst the reconsolidation of clay occurs around the pile, the high

positive pore pressures are diminished that leads to an increase in shear strength and pile capacity. The situation is opposite to “relaxation” phenomena. The zone and the magnitude of soil disturbance are affected by soil properties of soil sensitivity, driving method, and the pile foundation geometry.

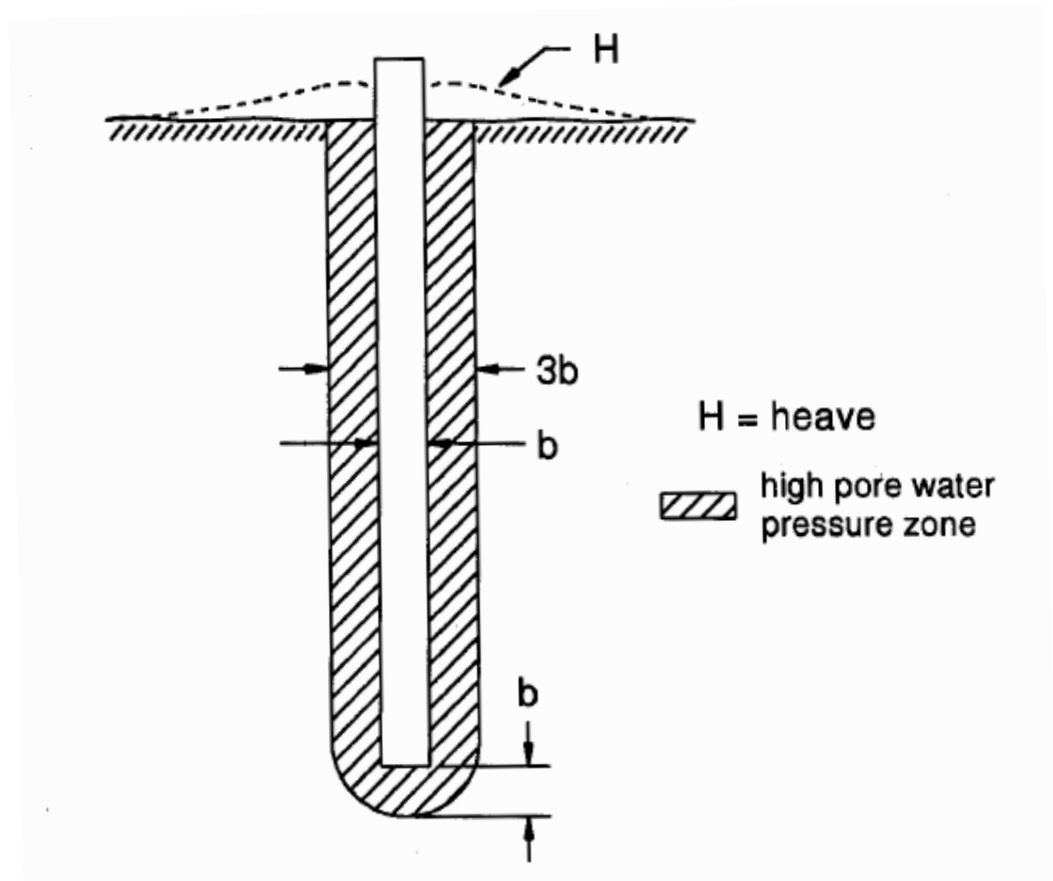


Figure 3.2 Disturbance of cohesive soils during driving of piles (Broms, 1966)

### 3.2. Load Transfer in Piles

Load is supported by two elements in piles. These are shaft resistance  $R_s$ , and toe resistance  $R_t$ . The ultimate bearing capacity can be expressed as:

$$Q_u = (f_s A_s) + (q_t A_t) \quad (3.2)$$

The first element in the brackets is shaft resistance, and the second element is toe resistance.  $f_s$  is the unit shaft resistance over the shaft surface area  $A_s$ , and  $q_t$  is the unit toe resistance over the pile toe area  $A_t$ . It is assumed that both pile toe and the pile shaft have

moved sufficiently with respect to the adjacent soil to simultaneously develop the ultimate shaft and toe resistances in the equation. In most cases the displacement needed to mobilize the shaft resistance is smaller than that required to mobilize the toe resistance. Figure 3.3 shows the typical load transfer profiles for a single pile and the measured axial load,  $Q_u$ , in the pile plotted against depth. Load transfer distribution can be obtained from a static load test where strain gages or telltale rods are attached to a pile at different depths along the pile shaft.  $R_s$  and  $R_t$  represents the resistance at the pile toe. In Figure 3.3.(a), the load transfer distribution for a pile with no shaft resistance is shown. In Figure 3.3.(b), the axial load versus depth for a uniform shaft resistance distribution typical of a cohesive soil is shown. In Figure 3.3.(c) the axial load in the pile versus depth for a triangular shaft resistance distribution which is typical for cohesionless soils is shown.

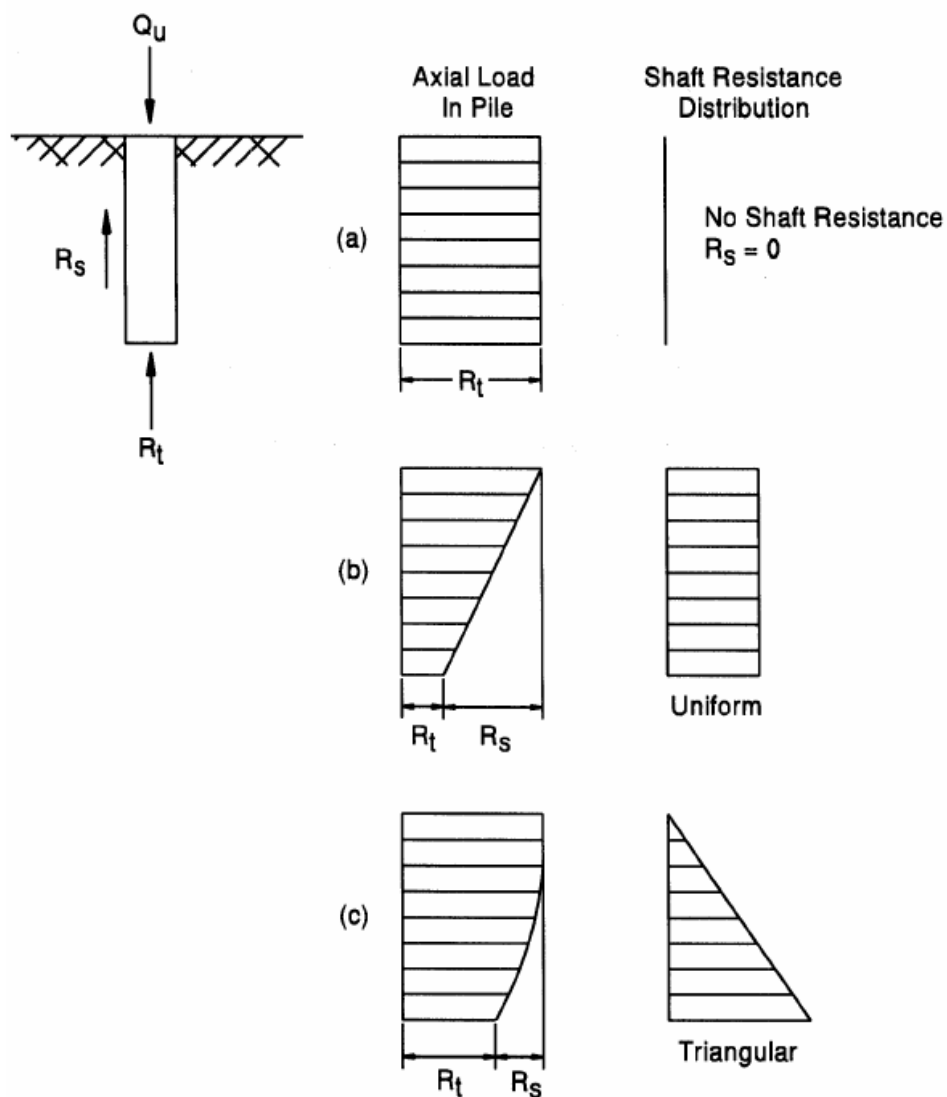


Figure 3.3 Typical load transfer profiles

## 4. INTRODUCTION TO PLAXIS

PLAXIS is a finite element package that has been developed specifically for the analysis of deformation and stability in geotechnical engineering projects. The simple graphical input procedures enable a quick generation of complex finite element models, and the enhanced output facilities provide a detailed presentation of computational results. The calculation process is fully automated and based on robust numerical procedures. This concept enables new users to work with the package after only a few hours of training.

Development of PLAXIS began in 1987 at the Technical University of Delft as an initiative of the Dutch Department of Public Works and Water Management. The initial brief was to develop an easy-to-use finite element code for the analysis of river embankments on the soft soils of the lowlands of Holland. In subsequent years, PLAXIS was extended to cover most other areas of geotechnical engineering. Because of continuously growing activities, a company named PLAXIS BV was formed in 1993. The program is intended to provide a practical analysis tool for use by geotechnical engineers who are not necessarily numerical specialists.

Geotechnical applications require advanced constitutive models for the simulation of the non-linear and time-dependent behavior of soils. Furthermore, since soil is a multi-phase material, special procedures are required to deal with hydrostatic and non-hydrostatic pore pressures in the soil. Although the modeling of the soil itself is an important issue, many geotechnical engineering projects involve the modeling of structures and the interaction between the structures and the soil. PLAXIS is equipped with special features to deal with the numerous aspects of complex geotechnical structures. Important features of the program can be given as:

- Graphical input of geometry models: The input of soil layers, structures, construction stages, loads and boundary conditions is based on convenient drawing procedures (CAD), which allows a detailed and accurate modeling of real situations to be achieved. From this geometry model a finite element mesh is automatically generated.

- Automatic mesh generation: PLAXIS allows for fully automatic generation of unstructured finite element meshes with options for global and local mesh refinement. The mesh generator is a special version of the Triangle generator, which was developed by Sepral.
- High-order elements: High order elements are available to enable a smooth distribution of stresses in the soil and an accurate prediction of failure loads. In addition to the quadratic 6-node triangular elements 15-node cubic strain triangles are available which perform extremely well in axisymmetric analyses.
- Beams: Special beam elements are used to model the bending of retaining walls, tunnel linings and other slender structures. The behavior of these elements is defined using a flexural rigidity, a normal stiffness and an ultimate bending moment. A plastic hinge may develop for elastoplastic beams, as soon as the ultimate moment is mobilized. Beams may be used together with interfaces to perform highly realistic analyses of a large range of geotechnical structures.
- Interfaces: These joint elements are needed for calculations involving soil-structure interaction. They may be used to simulate the thin zone of intensely shearing material at the contact of footings, piles, geotextiles, retaining walls, etc. Values of interface friction angle and adhesion that are not necessarily the same as the friction angle and cohesion of the surrounding soil may be assigned to these elements.
- Anchors: Elastoplastic spring elements are used to model anchors and struts. The behavior of these elements is defined using a normal stiffness and a maximum force. A special option exists for the analyses of pre-stressed (ground) anchors and excavation supports.
- Geotextiles: Geotextiles or geogrids are often used in practice for the construction of reinforced embankments or retaining soil structures. They can be simulated in PLAXIS by the use of special tension elements. It is often convenient to combine these elements with interfaces to model the interaction with the surrounding soil.
- Tunnels: PLAXIS offers a convenient option to create circular and non-circular tunnels composed of arcs. Beams and interfaces may be added to model the tunnel lining and the interaction with the surrounding soil. Fully isoparametric elements are used to model the curved boundaries within the mesh. Different practical methods are implemented to analyze the deformations that occur due to the construction of the tunnel.

- Mohr-Coulomb model: This robust and simple non-linear model is based on soil parameters that are known in most practical situations. Not all non-linear features of soil behavior are included in this model, however. The Mohr-Coulomb model may be used to compute realistic ultimate loads for circular footings, short piles, etc. It may also be used to calculate a safety factor using a 'phi-c reduction' approach.
- Advanced soil models: PLAXIS offers a variety of soil models in addition to the Mohr-Coulomb model. To analyze accurately the logarithmic compression behavior of normally consolidated soft soils, a Cam-Clay type model is available. This is referred to in this manual as the Soft Soil Model. An improved version of this model also includes the modeling of secondary compression (creep). For stiffer soils, such as over consolidated clays and sand, an elastoplastic type of hyperbolic model is available, which is called the Hardening Soil model. More detailed information on these models can be found in the Material Models Manual.
- Steady state pore pressure: Two alternative approaches exist for the generation of steady state pore pressures. Complex pore pressure distributions may be generated on the basis of a two-dimensional groundwater flow analysis. As an alternative for simpler situations, multi-linear pore pressure distributions can be directly generated on the basis of phreatic lines.
- Excess pore pressures: PLAXIS distinguishes between drained and undrained soils to model permeable sands as well as almost impermeable clays. Excess pore pressures are computed during plastic calculations when undrained soil layers are subjected to loads. Undrained loading situations are often decisive for the stability of geotechnical structures. In cases of insufficient stability, intermediate consolidation periods have to be introduced to reduce the excess pore pressures.
- Automatic load stepping: PLAXIS can be run in an automatic step-size and automatic time step selection mode. This avoids the need for users to select suitable load increments for plastic calculations by themselves and it guarantees an efficient and robust calculation process.
- Arc-length control: This feature enables accurate computations of collapse loads and failure mechanisms to be carried out. In conventional load-controlled calculations the iterative procedure breaks down as soon as the load is increased

beyond the peak load. With arc-length control, however, the applied load is scaled down to capture the peak load and any residual loads.

- Staged construction: It is possible to simulate construction and excavation processes by activating and deactivating clusters of elements. This procedure allows for a realistic assessment of stresses and displacements as caused, for example, by the construction of an earth dam or an excavation for a deep basement.
- Updated Lagrangian analysis: Using this option the finite element mesh is continuously updated during the calculation. For some situations, a conventional small strain analysis may show a significant change of geometry. In these situations it is advisable to perform a more accurate Updated Lagrangian calculation, which is called an Updated Mesh analysis in PLAXIS.
- Consolidation: The decay of excess pore pressures with time can be computed in a consolidation analysis. A consolidation analysis requires the input of permeability coefficients in the various soil layers. Automatic time stepping procedures make the analysis robust and easy to use.
- Safety factors: The factor of safety is usually defined as the ratio of the failure load to the working load. This definition is suitable for foundation structures, but not for embankments and sheet-pile walls. For this latter type of structure it is more appropriate to use the soil mechanics definition of a safety factor, which is the ratio of the available shear strength to the minimum shear strength needed for equilibrium. PLAXIS can be used to compute this factor of safety using a 'phi-c reduction' procedure.
- Presentation of results: The PLAXIS postprocessor has enhanced graphical features for displaying computational results. Exact values of displacements, stresses and structural forces can be obtained from the output tables. Plots and tables can be sent to output devices or can be exported to other software.
- Stress paths: A special tool is available for drawing load-displacement curves, stress paths and stress-strain diagrams. Particularly the visualization of stress paths provides a valuable insight into local soil behavior and enables a detailed analysis of the results of a PLAXIS calculation.

## 4.1. General Modeling Aspects

For each new project to be analyzed it is important to create a geometry model first. A geometry model is a representation of a real problem and consists of points, lines and clusters. A geometry model should include a representative division of the subsoil into distinct soil layers, structural objects, construction stages and loadings. The model must be sufficiently large so that the boundaries do not influence the results of the problem to be studied. The three types of components in a geometry model are described below in more detail.

### Points:

Points form the start and end of lines. Points can also be used for the positioning of anchors, point forces, point fixities and for local refinements of the finite element mesh.

### Lines:

Lines are used to define the physical boundaries of the geometry, the model boundaries and discontinuities in the geometry such as sheet pile walls, separations of distinct soil layers or construction stages. A line can have several functions or properties.

### Clusters:

Clusters are areas that are fully enclosed by lines. PLAXIS automatically recognizes clusters based on the input of geometry lines. Within a cluster the soil properties are homogeneous. Hence, clusters can be regarded as parts of soil layers. Actions related to clusters apply to all elements in the cluster. After the creation of a geometry model, a finite element model can automatically be generated, based on the composition of clusters and lines in the geometry model.

### 4.1.1. Components of Mesh

In a finite element mesh three types of components can be distinguished, as described below.

Elements:

During the generation of the mesh, clusters are divided into triangular elements. The default triangular element is the 6-node element. In addition, 15-node triangles are available for a more accurate calculation of stresses and failure loads (particularly for axisymmetric geometries). Considering the same element distribution (for example a default mesh generation) the user should be aware that meshes composed of 15-node elements are actually much finer and much more flexible, but calculations with these meshes are also much more time consuming than calculations with 6-node elements.

Nodes:

A 15-node triangle consists of 15 nodes and a 6-node triangle is defined by 6 nodes. The distribution of nodes over the elements is shown in Fig. 4.1. During a finite element calculation, displacements are calculated at the nodes. Nodes may be pre-selected for the generation of load-displacement curves.

Stress points:

In contrast to displacements, stresses are calculated at individual Gaussian integration points (or stress points) rather than at the nodes. A 15-node triangular element contains 12 stress points as indicated in Fig. 4.1. and a 6-node triangular element contains 3 stress points as indicated in Fig. 4.1. Stress points may be pre-selected for the generation of stress paths or stress-strain diagrams.

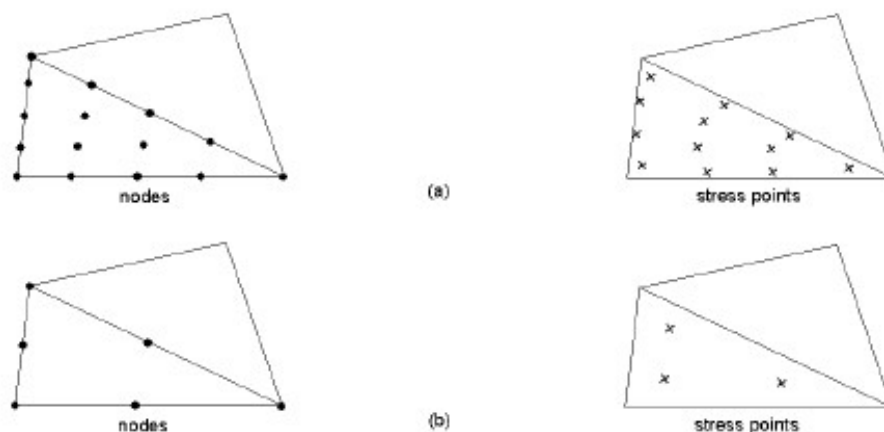


Figure 4.1. Stress points and nodes for a finite triangle element

## 5. SIMULATION OF MODEL

In the project an axisymmetric 15-node element model was used. In the manual of the program, it is strongly recommended to use 15-node element model for this kind of axisymmetric designs.

### 5.1. Mesh Generation

The mesh generator of the program requires a general meshing parameter which represents the average element size,  $l_e$ . In PLAXIS this parameter is calculated from the outer geometry dimensions ( $x_{\min}$ ,  $x_{\max}$ ,  $y_{\min}$ ,  $y_{\max}$ ) and a “Global Coarseness” setting as defined in the “Mesh” sub-menu:

$$l_e = \sqrt{\frac{(x_{\max} - x_{\min})(y_{\max} - y_{\min})}{n_c}} \quad (5.1)$$

Distinction is made between five levels of global coarseness: “Very coarse, Coarse, Medium, Fine, Very fine”. By default, the global coarseness is set to “Coarse”. The average element size and the number of generated elements depend on this global coarseness setting. A rough estimate is given below (based on a generation without local refinement):

Table 5.1. Global Coarseness Levels

Mesh Coarseness	Number of elements (Approximately)	$n_c$
Very coarse	50	25
Coarse	100	50
Medium	250	100
Fine	500	200
Very fine	1000	400

The exact number of elements depends on the exact geometry and eventual local refinement settings. The number of elements is not influenced by the “Type of elements parameter”, as set in the “General settings”. Note that a mesh composed of 15-node elements gives a much finer distribution of nodes and thus much more accurate results than a similar mesh composed of the same number of 6-node elements. On the other hand, the use of 15-node elements is much more time consuming than using 6-node elements. The inner part of the pile was graded to four parts to understand the effect of plugging.

Simulation was repeated with different mesh coarsenesses. For this model it is understood that the difference in deformation due to mesh coarseness is varies slightly. Because of this result, “medium” mesh coarseness was used to optimize the both processing time and reliability. Figures below show the different coarsenesses. Figure 5.1. for “Coarse Mesh”, Figure 5.2. for “Medium Mesh”, Figure 5.3. for “Very Fine Mesh” model. A uniformly distributed load was used both for inner part of the pile and neighborhood of the pile to prevent tension cracks. The magnitude of uniformly distributed load was 3 kN/m. The magnitude was chosen so that no influence on deformation will be created.

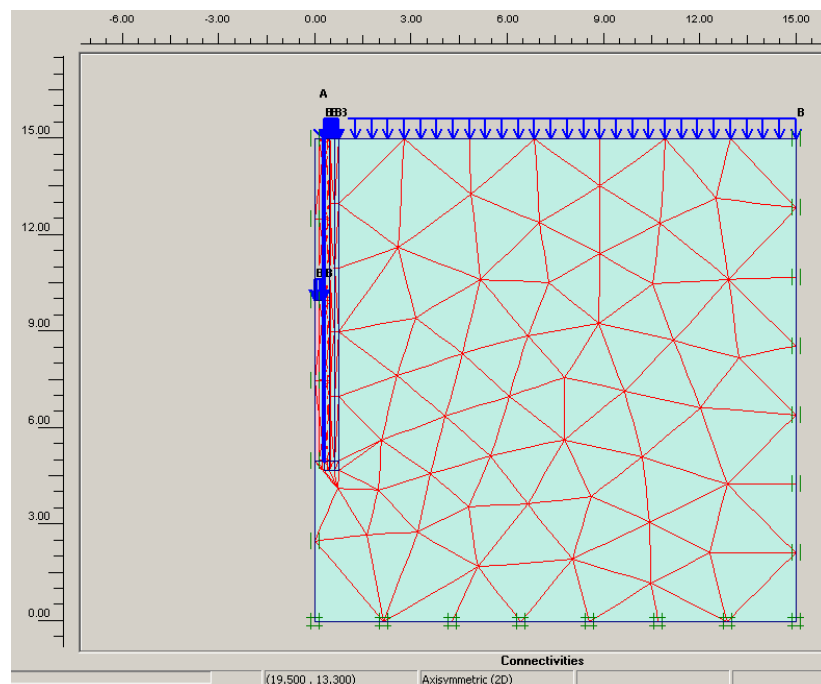


Figure 5.1. Coarse Mesh

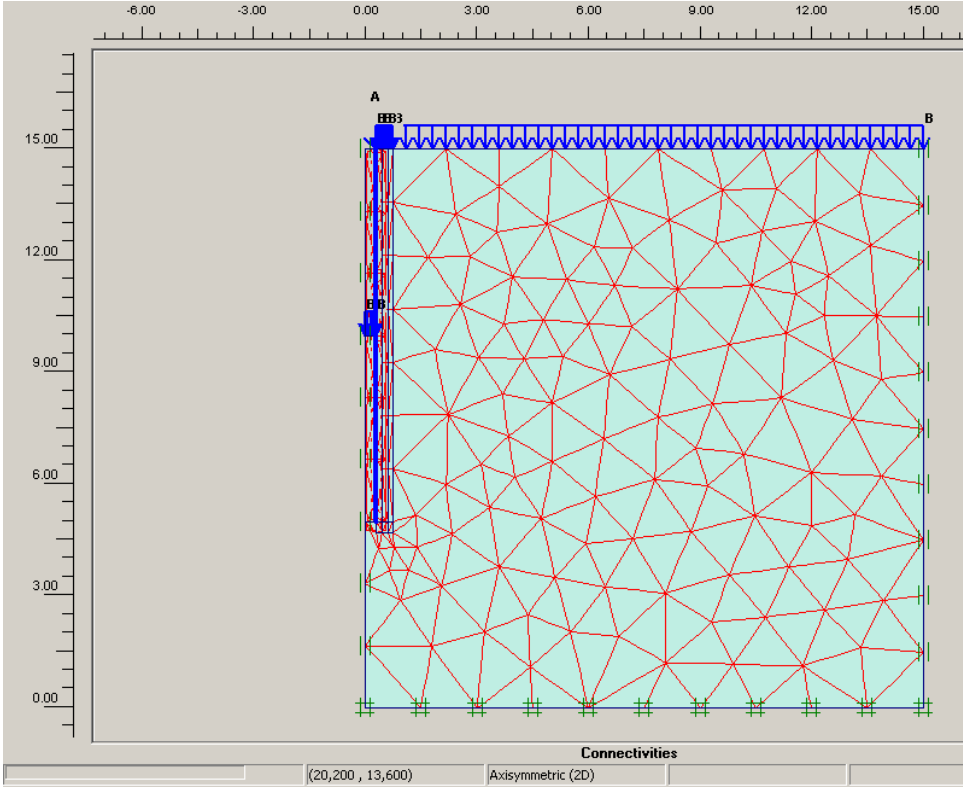


Figure 5.2. Medium Mesh

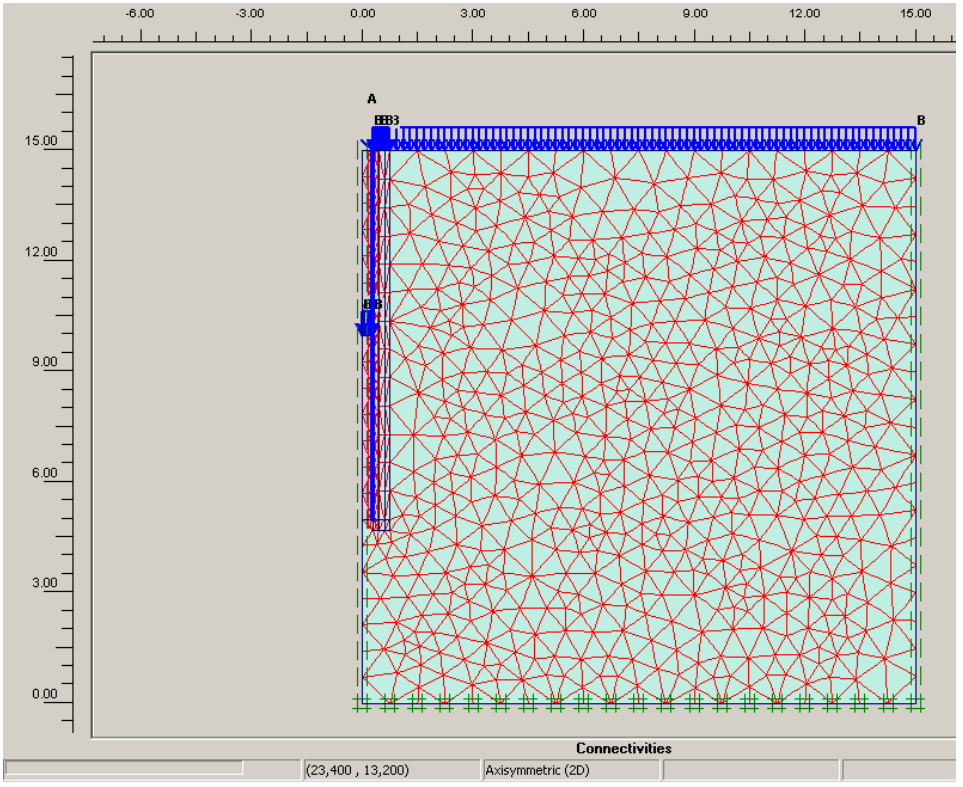


Figure 5.3. Very Fine Mesh

Soils with different properties were used in simulation. According to the type of problem, all of the soil types used in the simulation were cohesionless. Soils with different interface parameters, lateral earth pressures ( $K_0$ ), elasticities and internal friction angles were tested in simulation. The effect of ground water is not discussed in this thesis. Due to this situation and the deprivation of ground water, permeabilities were chosen as adjacent to zero. In the simulation of the pile, “Elastic Model” was used. The elasticity of pile was chosen as standard construction steel. The moment of inertia and area of pile were calculated as below:

Properties of pile:

$$\text{Perimeter} = \pi \times D = \pi \times 0.6 = 1.88495m$$

$$\text{Diameter} = 0.6m$$

$$E = 2.1 \times 10^6 N / mm^2$$

$$A = \frac{\pi(d^2 - d_1^2)}{4} = 185.35396 \times 10^{-4} m^2$$

$$I = \frac{\pi(d^4 - d_1^4)}{64} = 0.806753 \times 10^{-4} m^4$$

The load applied by the PLAXIS was a ring load. This means the load applied in the model was a radial unit load. The exact load can be calculated by multiplying the perimeter of pile with ring load. In the model the diameter of the pile was 0,6m. So according to the explanation above, the actual loads on pile were the multiplication of 1.885 with 100 kN, 200 kN, 300 kN, 400 kN, 500 kN which are 189 kN, 378 kN, 567 kN, 756 kN, 945 kN respectively. The Figure 5.4.(a) shows the radial ring load on the steel pile.

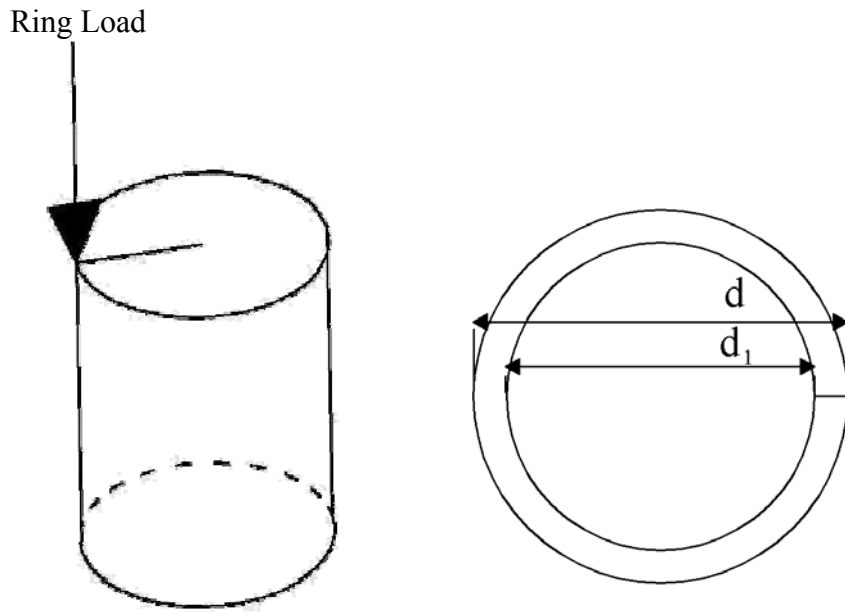


Figure 5.4 The “Ring Load” (a) and Pile Cross section (b)

The coefficient for lateral earth pressure  $K_0$  was incrementally varied towards the pile body. Meyerhoff tables were used to determine the point where increase of lateral pressure will start. These intervals also show the range of  $K_0$ , and the distance between the increment points. The varying lateral earth pressures varied in three steps. The number of steps was not increased not to affect process time undesirably. Figure 5.5. shows the magnitude of influence area and chosen “ $K_0$  varying” intervals.

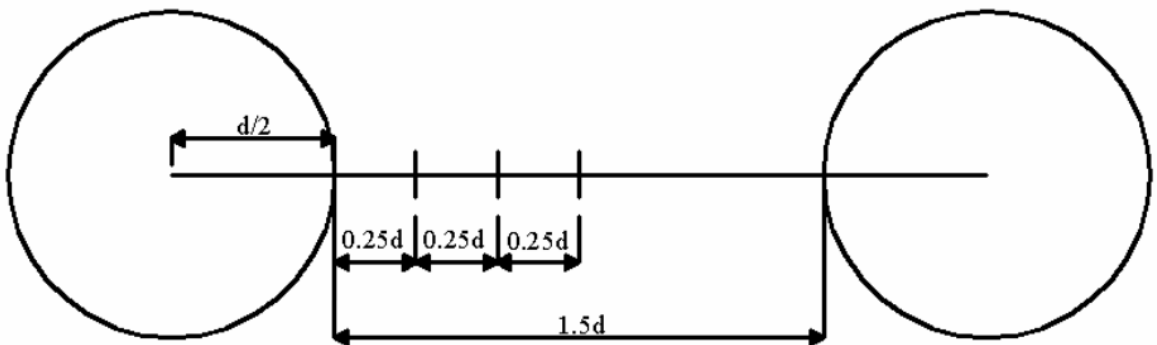


Figure 5.5. Distance of influence for piles and chosen “ $K_0$  intervals”

Naturally soil does not bear tension forces. Due to this characteristic, tensile effects must be eliminated. This option can be done by ticking off the “tension cut-off box” in the “advanced” section under “soil parameters tab” of the “material sets” menu. But on behalf of being on safe side, negligible distributed loads were used both for the inner part and neighborhood of the pile. Figure 5.6. shows the uniformly distributed insignificant loads.

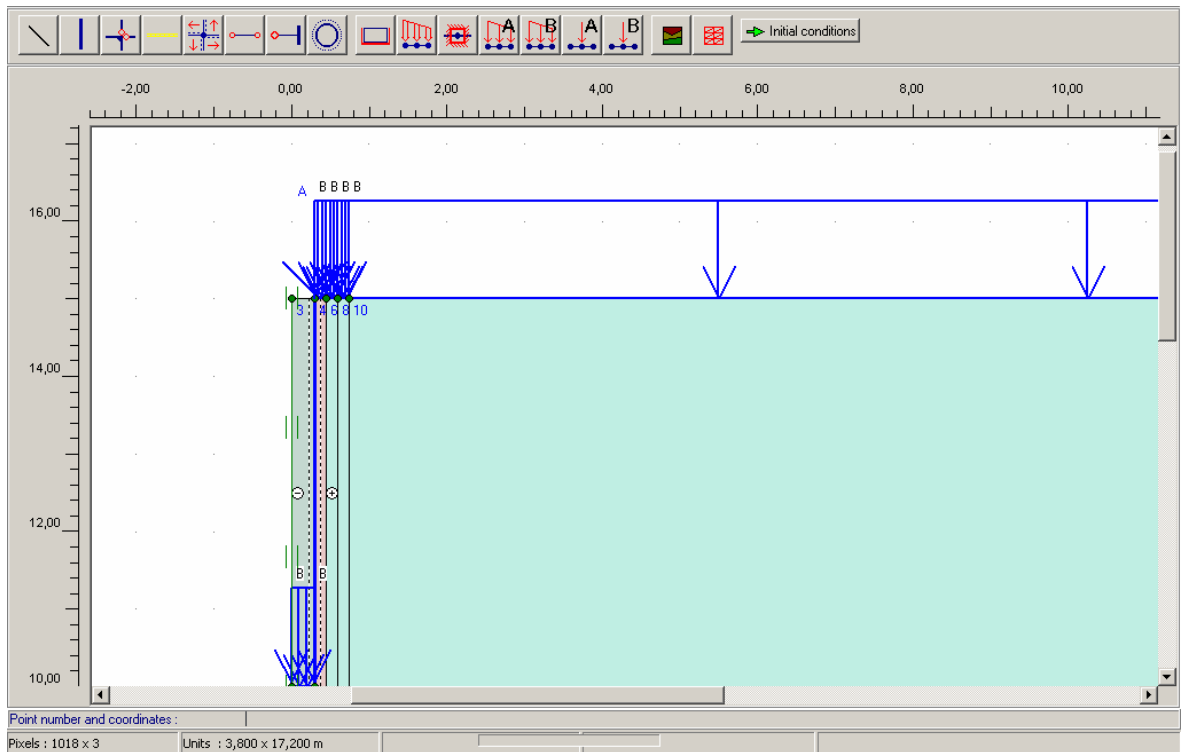


Figure 5.6. Negligible distributed loads preventing tension cracks

The interface line was firstly modeled as finishing with the end of steel pile. But considering the load accumulation at the toe of pile, the interface line is extended “radius of pile” unit, for a more realistic simulation. In the Figure 5.7. below, the extended interface can be seen. Here, also the intervals for varying  $K_0$  lateral earth pressure can be seen clearly.

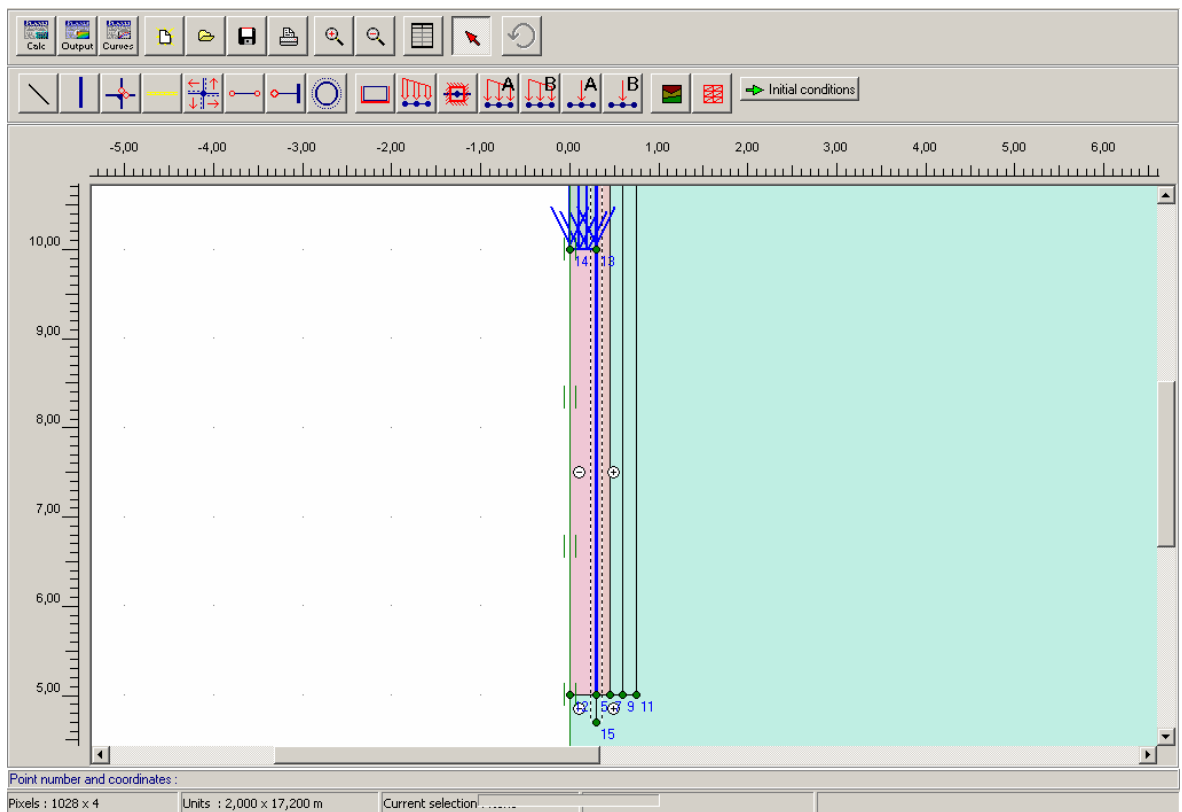


Figure 5.7. Extended interface and varying  $K_0$ 's

According to PLAXIS's finite element method, when a soil body is "deactivated" during the calculation steps, the massive soil body under the "deactivated" section starts to shrink and move upwards. This kind of solution may give false settlement values especially if the "deactivated" section is in the inner part of the steel pipe. To prevent this situation, and improve the simulation, weight of soil in the inner side of pile is valued as close to zero. With the "zero" weight of the removed soil in the inner side, "deactivating" has no effect on settlement and deformation of the whole system. Figure 5.8. shows the deformation with a weighted soil, and Figure 5.9. shows the deformation when a "weightless" soil section is used. The ratio between "weighted" and "weightless" state is 10 times. In Figure 5.8., it can be obviously seen that the soil section under the removed part may mislead us when deformed mesh is compared to initial model.

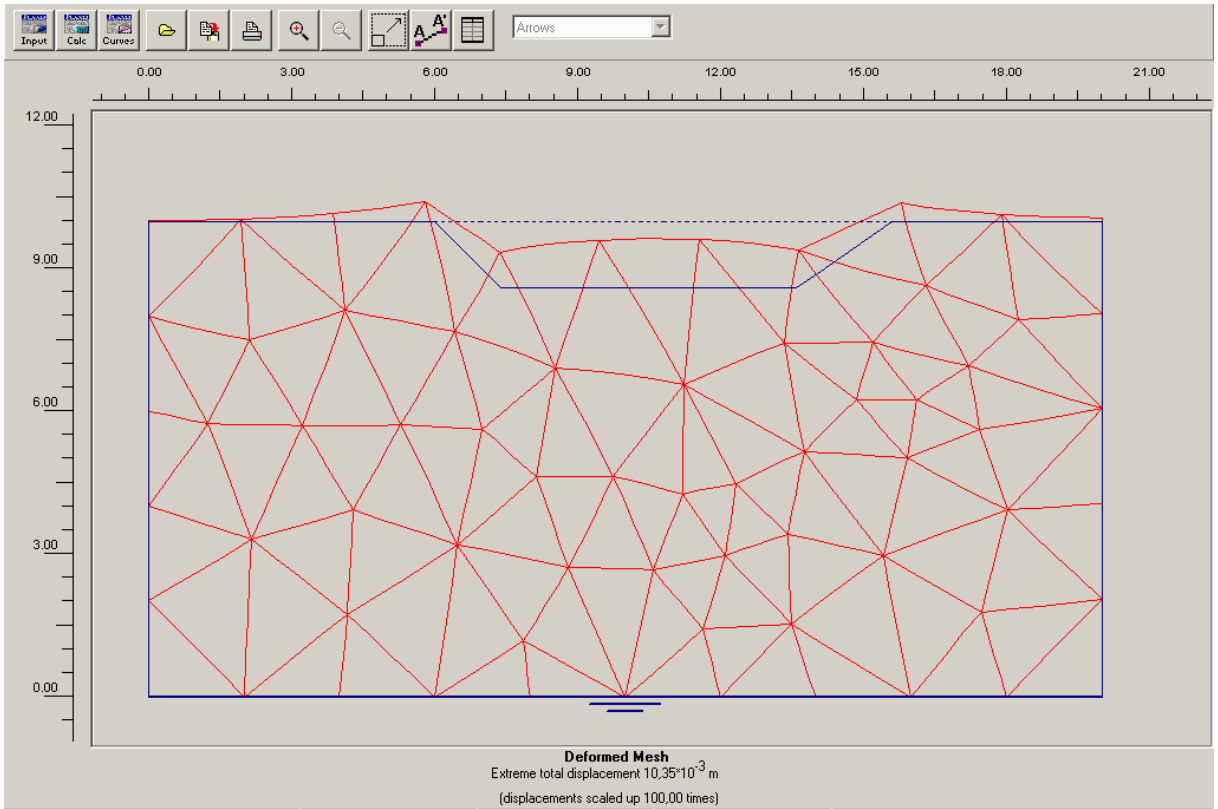


Figure 5.8. Deformation with a weighted soil

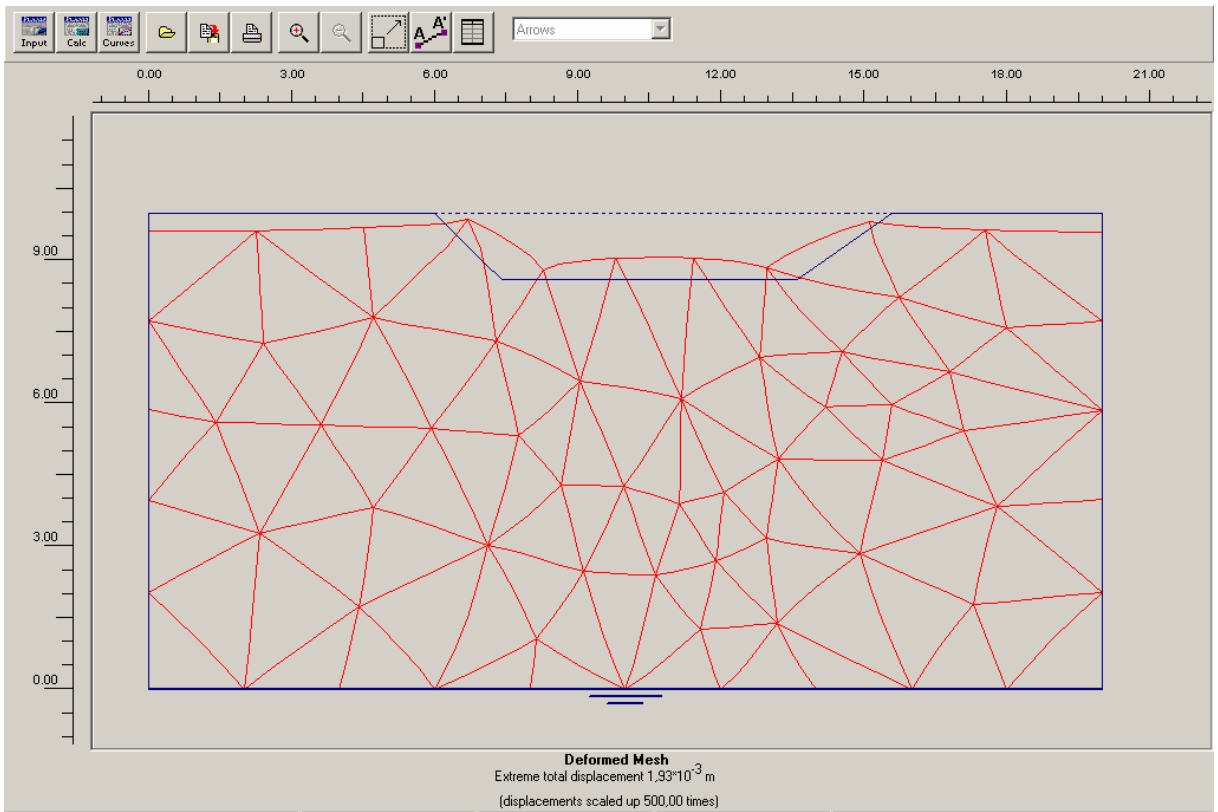


Figure 5.9. Deformation when a “weightless” soil section is used

In our simulation there is no soil in upper part of pile. Initial model is designed with no soil inside, and the probable “plugging” will occur after some penetrating of the pile to the soil. After the geometry was built, mesh was generated, soils were defined, and both point and distributed loads are imposed, the modeling is completed. Figure 5.10. shows the final design of the simulation model.

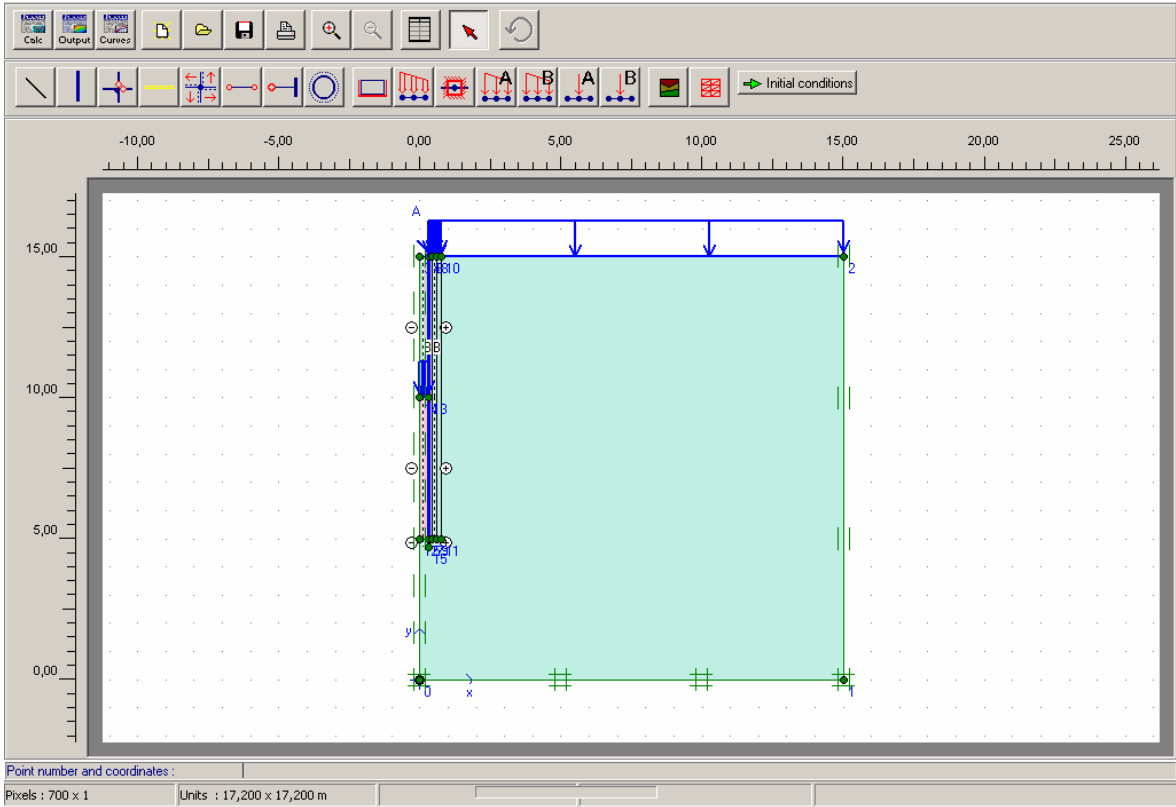


Figure 5.10. Complete simulation model

The soil properties used in PLAXIS is shown below:

Table 5.2. Soil properties

Parameter	Symbol	Sand	3xE Sand	5xE Sand	Unweighed Sand	Unit
Material Model	Model	Mohr-Coulomb	Mohr-Coulomb	Mohr-Coulomb	Mohr-Coulomb	-
Type of Behavior	Type	Drained	Drained	Drained	Drained	-
Young's Modulus	$E_{ref}$	13000	39000	65000	13000	$\text{kN/m}^2$
Unit Weight above phreatic line	$\gamma_{dry}$	17	17	17	$1 \times 10^{-5}$	$\text{kN/m}^3$
Unit Weight below phreatic line	$\gamma_{wet}$	20	20	20	$1 \times 10^{-5}$	$\text{kN/m}^3$
Permeability x direction	$k_x$	-	-	-	-	m/d
Permeability y direction	$k_y$	-	-	-	-	m/d

## 5.2. Manual Calculation of Bearing Capacity:

To express the manual calculation clearly, a problem with adjacent characteristics is solved below:

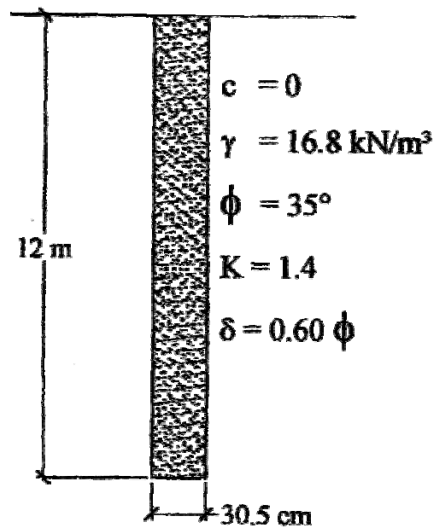


Figure 5.11. Pile problem

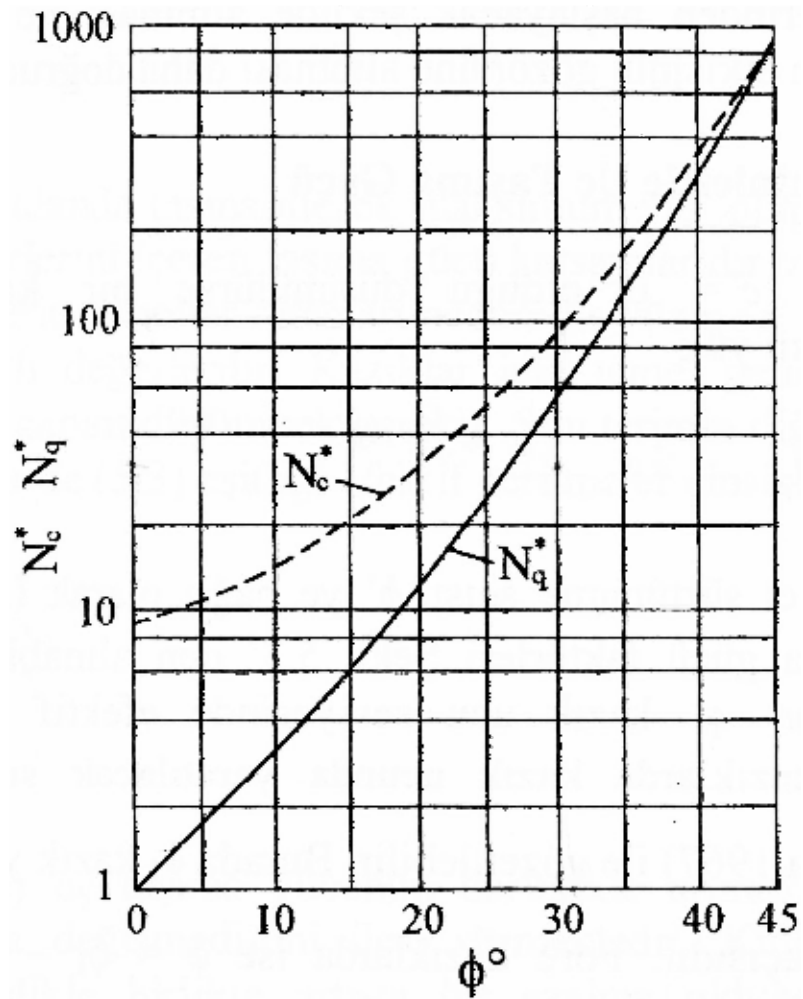


Figure 5.12. Bearing capacity factor  $N_q^*$  in granular soils (Meyerhof 1976)

The manual calculation of ultimate capacity of a pile in cohesionless soil can be derived by:

$$\phi = 35^\circ$$

$$N_q^* = 120 \quad (\text{From the Meyerhof table})$$

$$Q_u = Q_p + Q_s$$

$$Q_p = q N_q^* A_p = (12 \times 16.8) \times 120 \times 0.093 = 2250 \text{ kN}$$

$q$  = effective vertical stress at the pile toe

Limit bearing capacity:

$$q_l = 50 \times N_q^* \times \tan \phi = 50 \times 120 \times \tan 35 = 4201.25 \text{ kN/m}^2$$

$$Q_{p\_LIMIT} = q_l A_p = 4201.25 \times 0.093 = 390.82 kN$$

$$Q_s = \Delta p \times \Delta l \times f$$

$$f = K \sigma'_v \tan \delta$$

$$Q_{s(0-4.75)} = 1.22 \times 4.575 \left( \frac{1.4 \times 78.86 \times \tan(0.6 \times 35)}{2} \right) = 118.27 kN$$

$$Q_{s(4.75-12)} = 1.22 \times 7.425 \times 1.4 \times 78.86 \times \tan(0.6 \times 35) = 383.90 kN$$

$$Q_s = 118.27 + 383.90 = 502.17 kN$$

$$Q_u = 390.82 + 502.17 = 892.99 kN$$

$$Q_a = \frac{892.99}{3} = 297.6 kN$$

If we apply the same formulas to our simulation problem, the results are:

$$A_p = 0.0185 m^2$$

$$Q_p = q N_q^* A_p = (20 \times 10) \times 75 \times 0.0185 = 277.5 kN$$

$$p = 1.885 m$$

$$f = K \sigma'_v \tan \delta$$

$$K = 1.5$$

$$\delta = 0.666 \times \phi = 31 \times \frac{2}{3}$$

$$Q_{s(0-9)} = 1.885 \times 9 \times \left( \frac{1.5 \times 153 \times \tan(0.666 \times 31)}{2} \right) = 733.513 kN$$

$$Q_{s(9-10)} = 1.885 \times 1 \times 1.5 \times 153 \times \tan(0.666 \times 31) = 163 kN$$

$$Q_s = 896.513 kN$$

$$Q_u = 277.5 + 896.513 = 1174.013 kN$$

With these coefficients and parameters, higher values of static load capacity are found in PLAXIS due to the manual calculation. Because of these results, searching for the “collapsing load” is preferred rather than examining the factor of safety results.

Table 5.3. Static load capacities due to the factor of safety values

Ring Load (kN)	Actual Load (kN)	Factor of Safety	Ultimate Load (kN)
100	189	8,49	1604,61
200	378	5,8	2192,4
300	567	4,75	2693,25
356	672	4,21	2829,12

## 6. RESULTS

Figure 6.1. shows the settlement of a 10 meter pile with different mesh coarsenesses in cohesive soil. The results show that “Medium” coarse mesh utilization is enough for both accuracy and processing time.

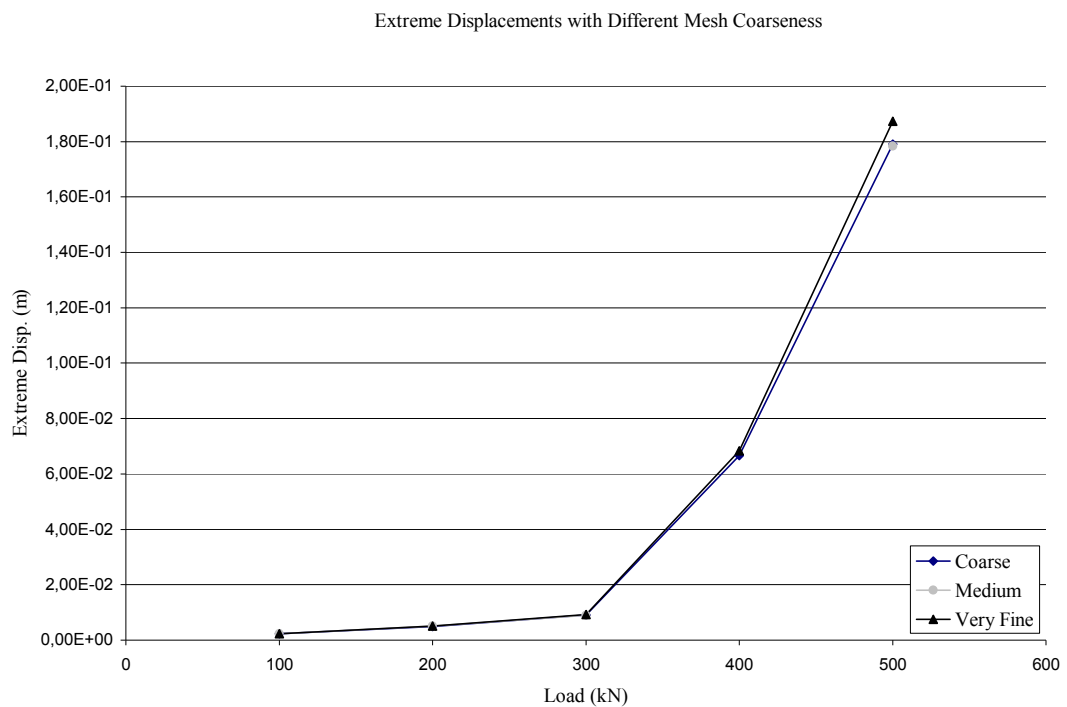


Figure 6.1. Settlements with different mesh coarsenesses

### 6.1. Factor of Safety Values

24 tests were conducted with the model. In two of the tests system collapsed. The “collapsed” tests are 400 kN ring load,  $\phi=31^{\circ}$ ,  $R_{\text{interface}}=0.5$  and 400 kN ring load,  $\phi=31^{\circ}$ ,  $R_{\text{interface}}=0.75$ . No figures are available for these tests in Appendix A. During the tests, different internal friction angles, interface coefficients and loads were executed. The figures for the test results are in Appendix A.

Table 6.1 Factor of safety values for different Young's Moduluses ( $\phi=31^\circ$ ,  $R_{\text{interface}}=0,666$ )

Ring Load (kN)	$E$	$3 \times E$	$5 \times E$
100	8,49	8,99	8,94
200	5,8	5,89	5,9
300	4,75	4,47	4,3
356	4,21	3,85	3,87

Factor of safety values with different soils (varying E parameters) are not varying widely. After these results, tests with different internal friction angles and interface parameters were conducted. The results are below:

Table 6.2. Factor of safety values with different interface coefficients

		$\Phi=31^\circ$	$\Phi=33^\circ$	$\Phi=35^\circ$
$R_{\text{interface}}$	Load	<i>Factor of Safety</i>	<i>Factor of Safety</i>	<i>Factor of Safety</i>
0,5	100kN	8,85	8,1	8,65
	200kN	6	5,9	6
	300kN	4,65	4,53	4,45
	400kN	Collapse (at 356 kN)	3,8	3,77
0,75	100kN	8	8,1	9,13
	200kN	5,95	6,12	6,18
	300kN	4,4	4,58	4,6
	400kN	Collapse (at 356 kN)	3,82	4,1

Due to the results of the tests, it is seen that factor of safety values follow a trend and these values are matching in between themselves. When small amounts of loads are installed, the ratios between factors of safety at different E values are not close. But with the increment of Ring load to the value of 300 and 400 kN, calculated ultimate loading capacities become more close and coherent.

When the system started to collapse at a value of approximately 350 kN, the model was changed. The rigidity of soil in the inner part of pile was increased to understand whether there is a contribution at bearing capacity or not. But the results show that there are no major changes in the factor of safety values due to varying E parameters. To understand the affect of varying E values, bearing capacity is inspected in the next steps. This time more coherent results were taken.

The insufficient results using FOS could occur because of the program itself. PLAXIS's calculating method for safety factors is shown below:

$$\Sigma Msf = \frac{c}{c_{reduced}} = \frac{\tan \phi}{\tan \phi_{reduced}} \quad (6.1)$$

Because of the small change in internal friction angle, tangent values and accordingly  $\Sigma Msf$  values change at very negligible values. This explains us the very small changes even when using elasticity three or five times the normal stiffness.

Other tests were conducted to investigate the ultimate load capacity of pile. Here, the internal friction angle and the stiffness were the varying parameters. Young's modulus of the soil which generates the perimeter of the pile toe is taken as three and five times bigger.

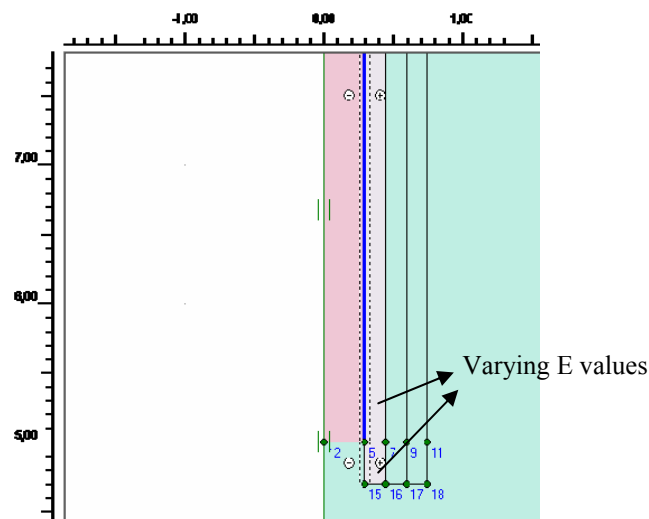


Figure 6.2. Varying stiffness values at right side of the pile

Table 6.3. Ultimate load capacities of piles (kN) under different soil parameters

Stiffness in Right Side of Pile, $R_{\text{interface}}=0.5$	Collapsing Values (kN)		
	$\Phi=31^\circ$	$\Phi=33^\circ$	$\Phi=35^\circ$
$3 \times E$	862	861	860
$5 \times E$	860	861	861

## 7. CONCLUSION

This study presented the bearing capacity of an open ended pile in a cohesionless soil with varying soil parameters. Load capacities of soils with different internal friction angles, Young's Modulus and soil cross section models were calculated. Not only was the load capacity, factor of safety coefficients also calculated by using PLAXIS. The effect of plugging were investigated and discussed by using finite element simulation program PLAXIS.

From the simulation tests, it is understood that plugging is not effective upon the load capacity. Different materials with varying modulus of elasticity values in the inner part of pile were used, and results show that load capacity does not vary in a wide range.

According to PLAXIS tests, the exact importance at the pile capacity was found as the modulus of elasticity of the region at the pile toe. With varying the parameters (internal friction angle, number of segments in pile and their thickness) test results show that the important and effective parameter is E (Young Modulus) at the pile toe. To derive a more realistic and reliable solution for pile load capacity problems, the toe region of the pile may be modeled "stiffer". With this "stiffer" region, mathematical solution of PLAXIS would not "collapse" in any part of the whole model under small loads, and with this "precaution" ultimate loads may be used to determine the capacity of pile.

**APPENDIX A: TEST RESULTS FOR FACTOR OF SAFETY VALUES**

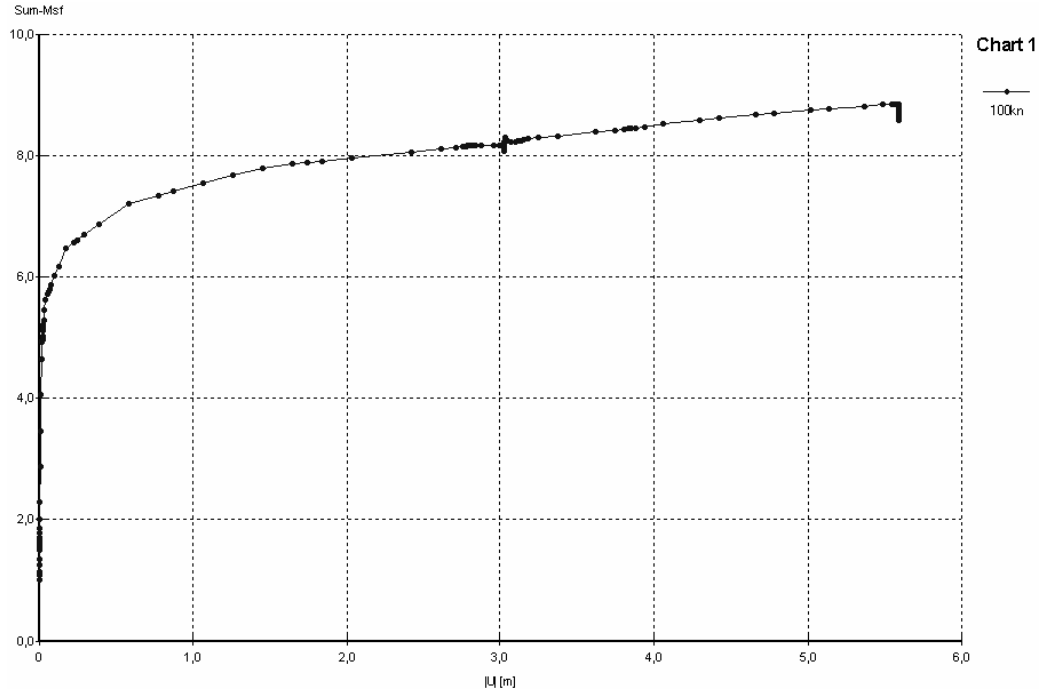


Figure A.1. Factor of safety with 100 kN ring load,  $\phi=31^{\circ}$ ,  $R_{\text{interface}}=0.5$

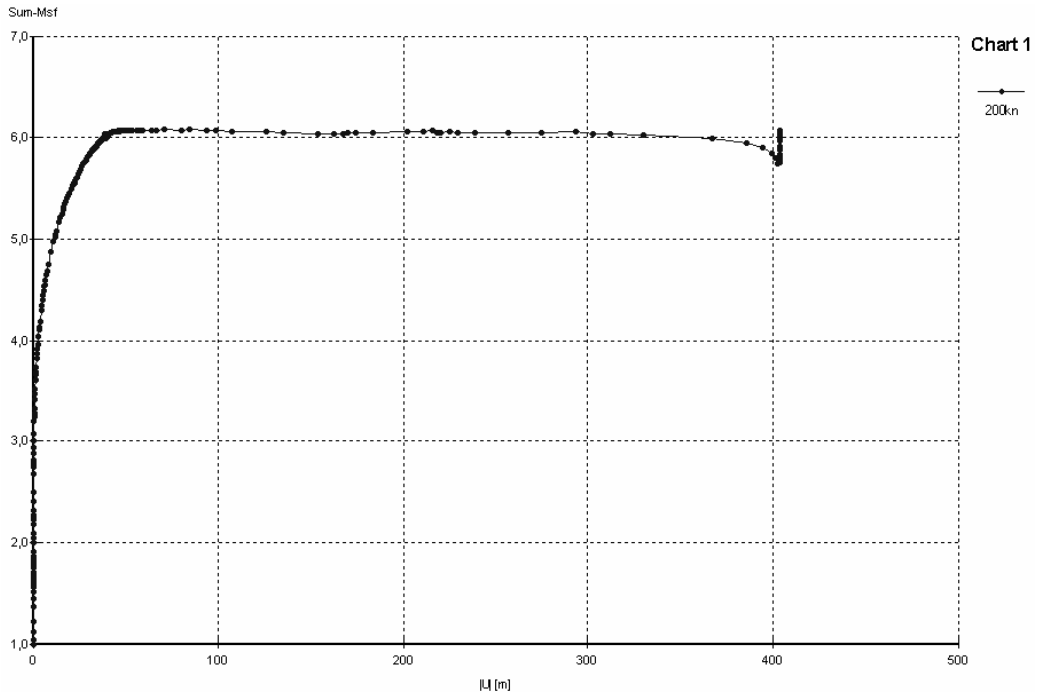


Figure A.2. Factor of safety with 200 kN ring load,  $\phi=31^{\circ}$ ,  $R_{\text{interface}}=0.5$

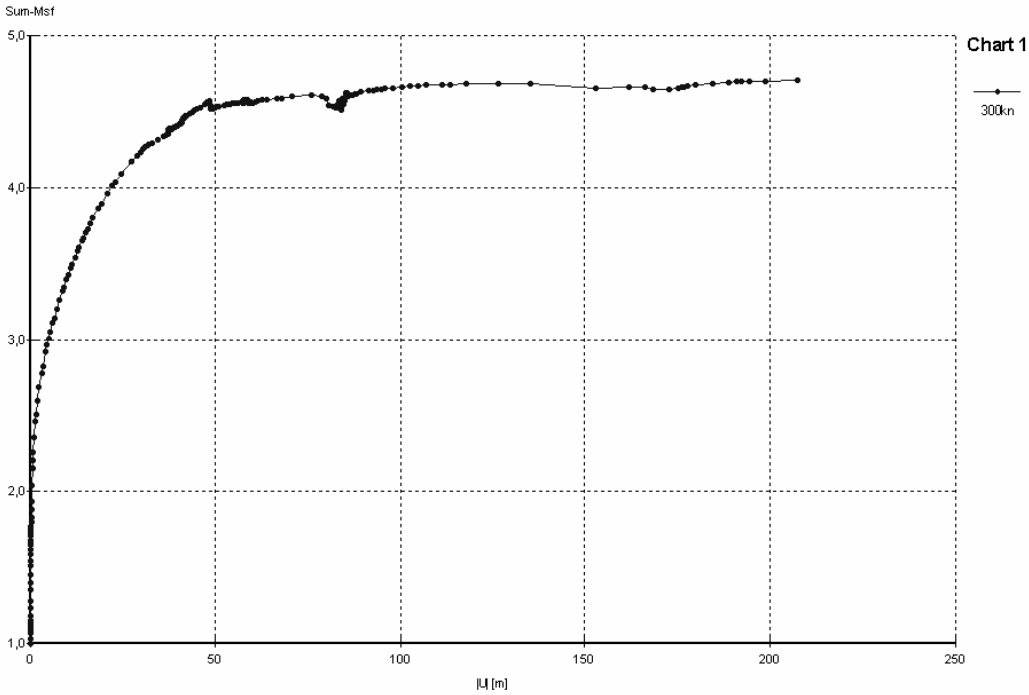


Figure A.3. Factor of safety with 300 kN ring load,  $\varphi=31^{\circ}$ ,  $R_{\text{interface}}=0.5$

The system collapsed when 400 kN load was applied. So there is no result of 400 kN with  $\varphi=31^{\circ}$  and 0.5 interface.

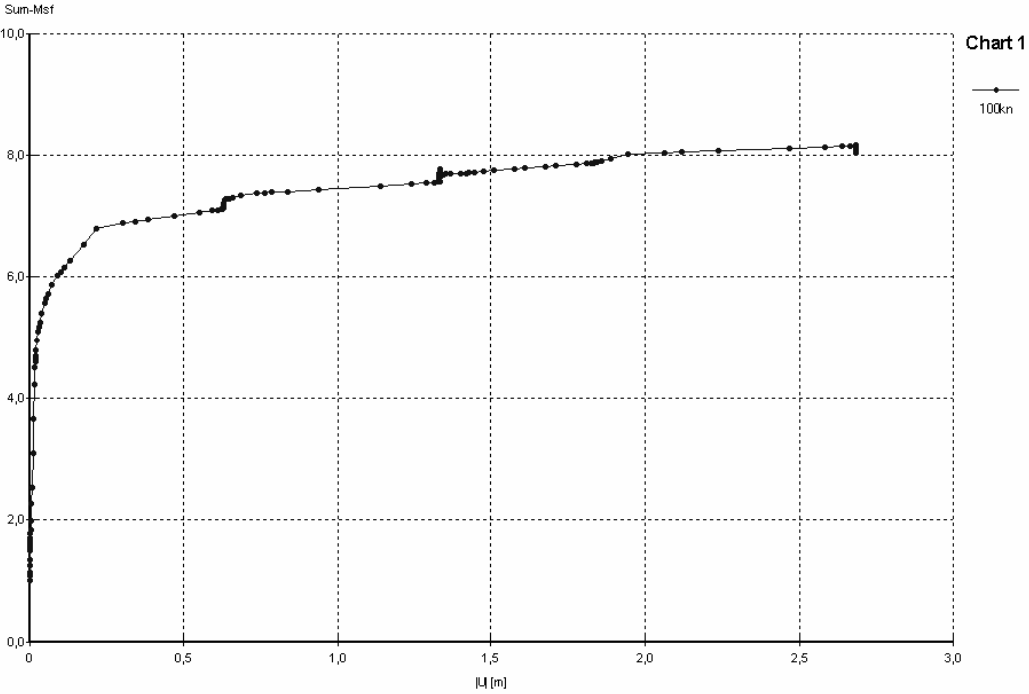


Figure A.4. Factor of safety with 100 kN ring load,  $\varphi=33^{\circ}$ ,  $R_{\text{interface}}=0.5$

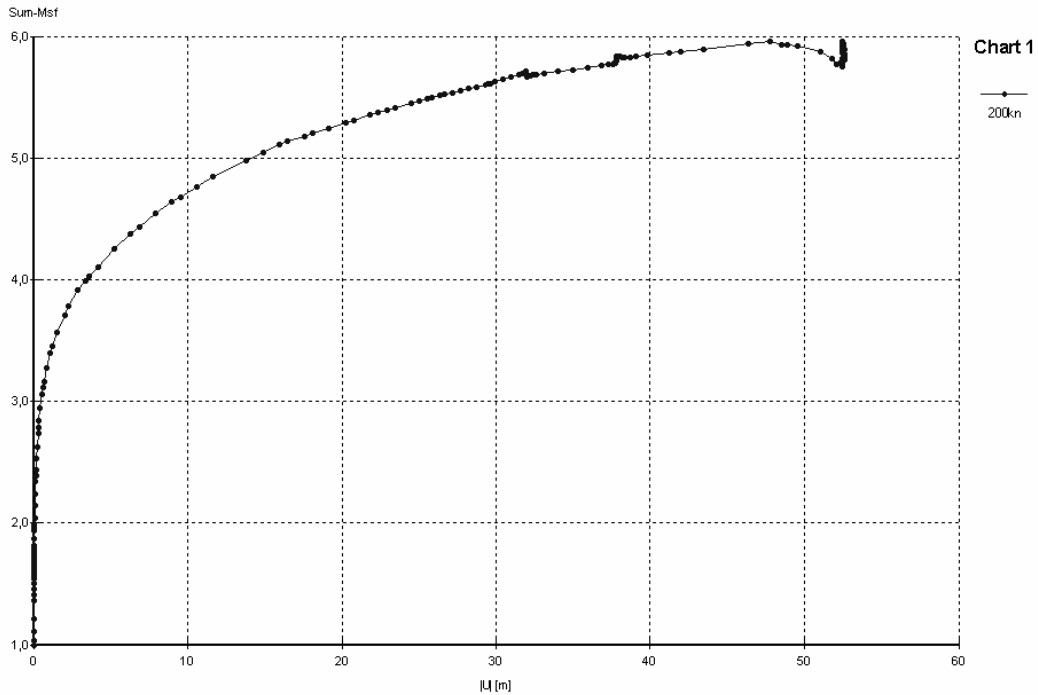


Figure A.5. Factor of safety with 200 kN ring load,  $\phi=33^{\circ}$ ,  $R_{\text{interface}}=0.5$

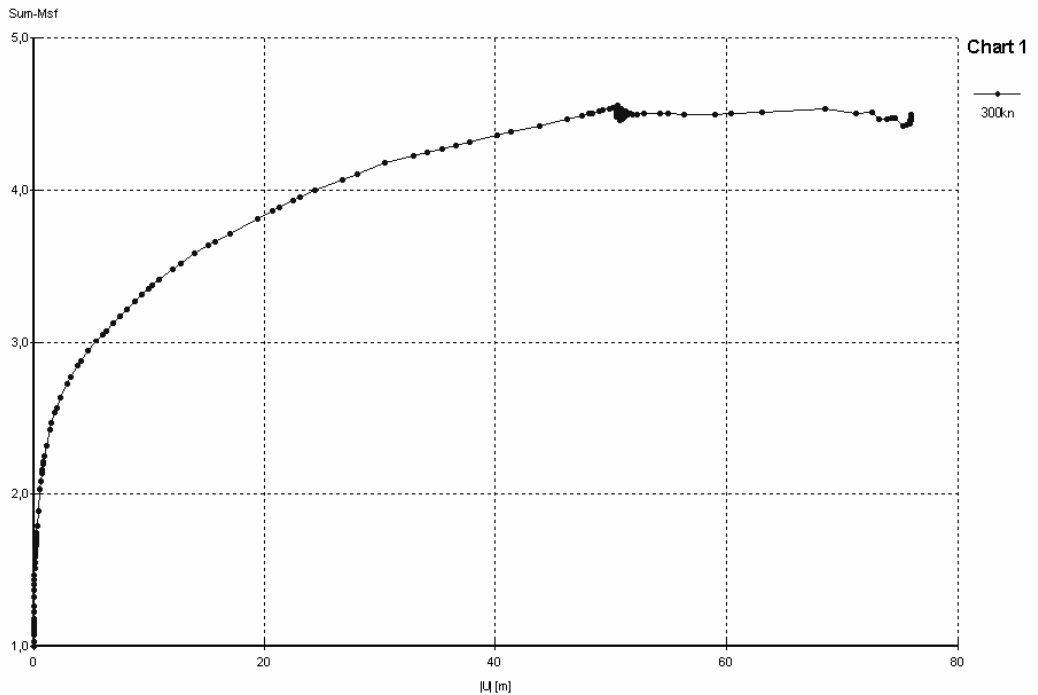


Figure A.6. Factor of safety with 300 kN ring load,  $\phi=33^{\circ}$ ,  $R_{\text{interface}}=0.5$

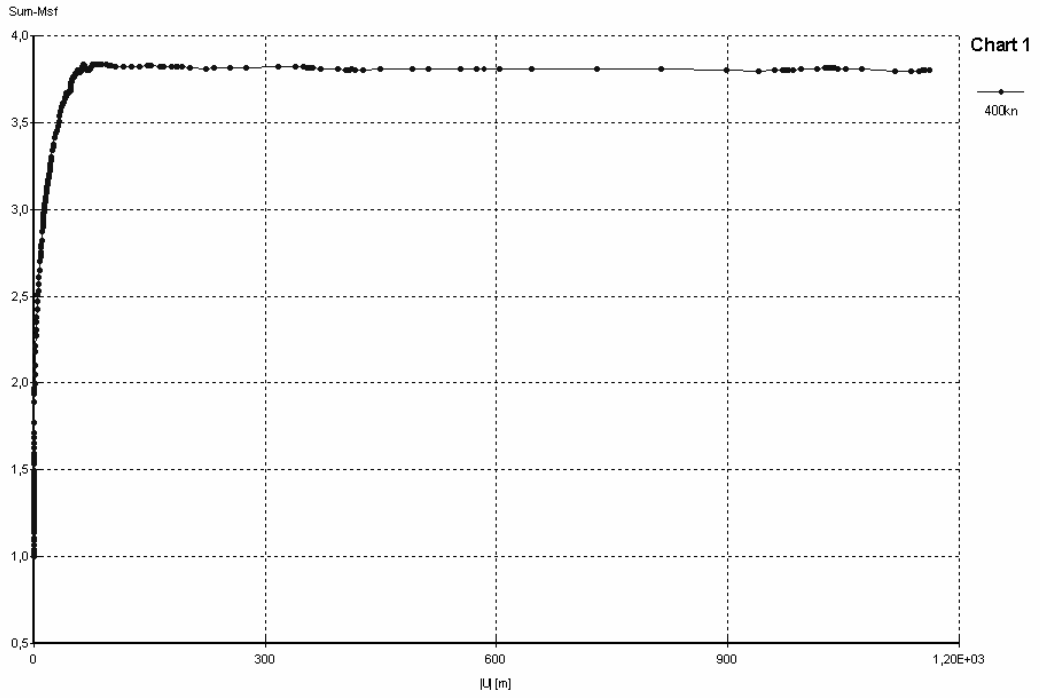


Figure A.7. Factor of safety with 400 kN ring load,  $\phi=33^{\circ}$ ,  $R_{\text{interface}}=0.5$

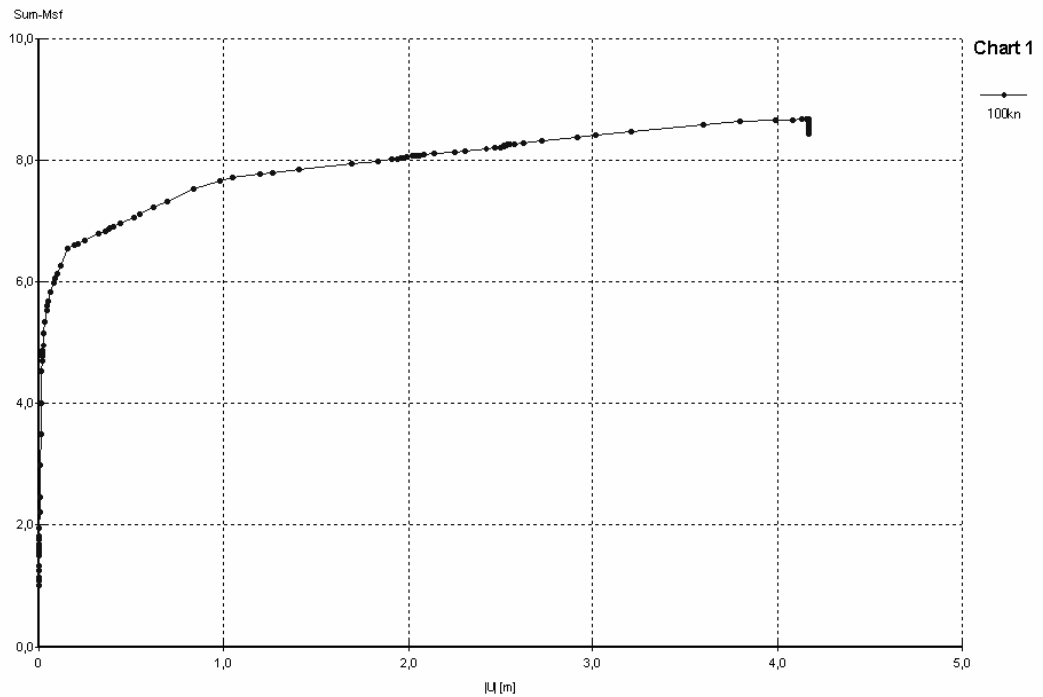


Figure A.8. Factor of safety with 100 kN ring load,  $\phi=35^{\circ}$ ,  $R_{\text{interface}}=0.5$

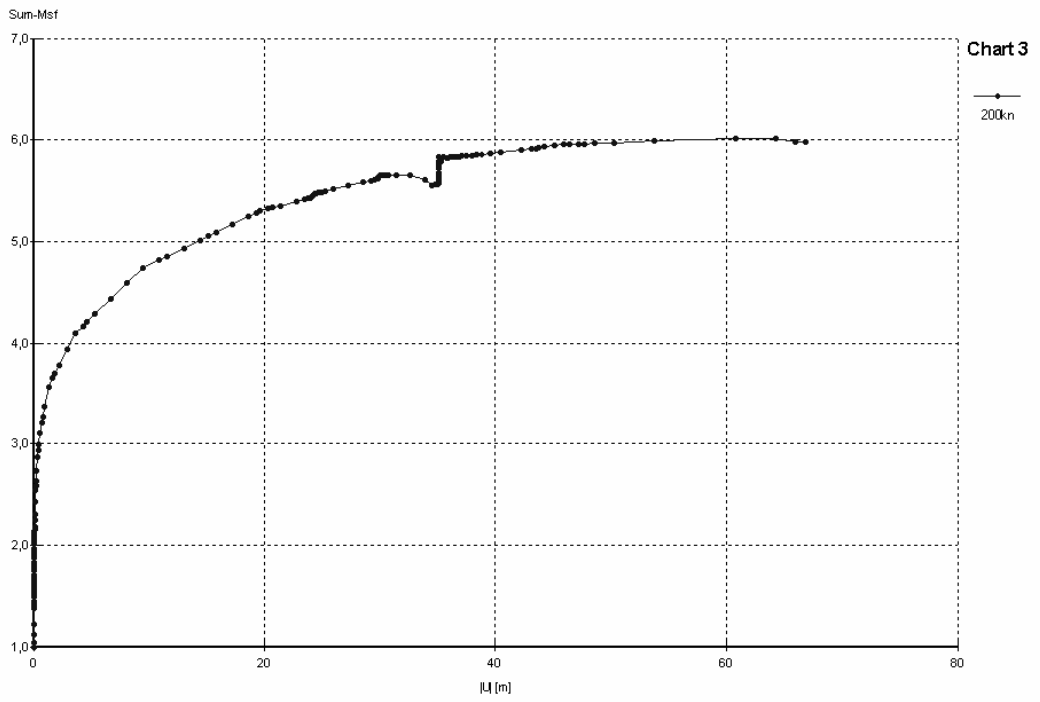


Figure A.9. Factor of safety with 200 kN ring load,  $\phi=35^0$ ,  $R_{interface}=0.5$

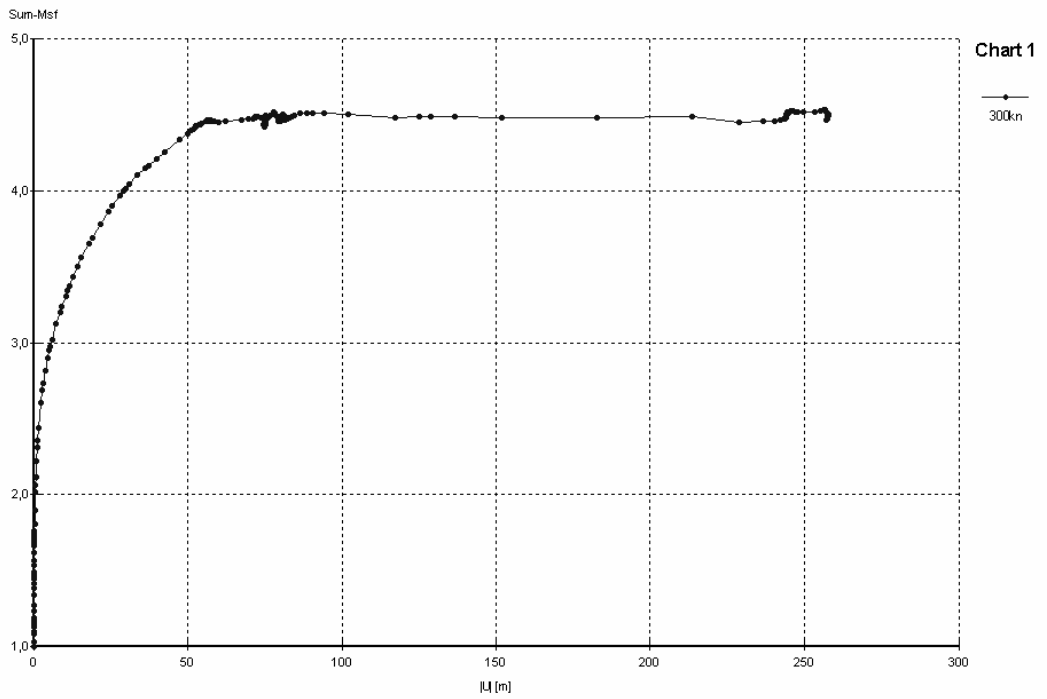


Figure A.10. Factor of safety with 300 kN ring load,  $\phi=35^0$ ,  $R_{interface}=0.5$

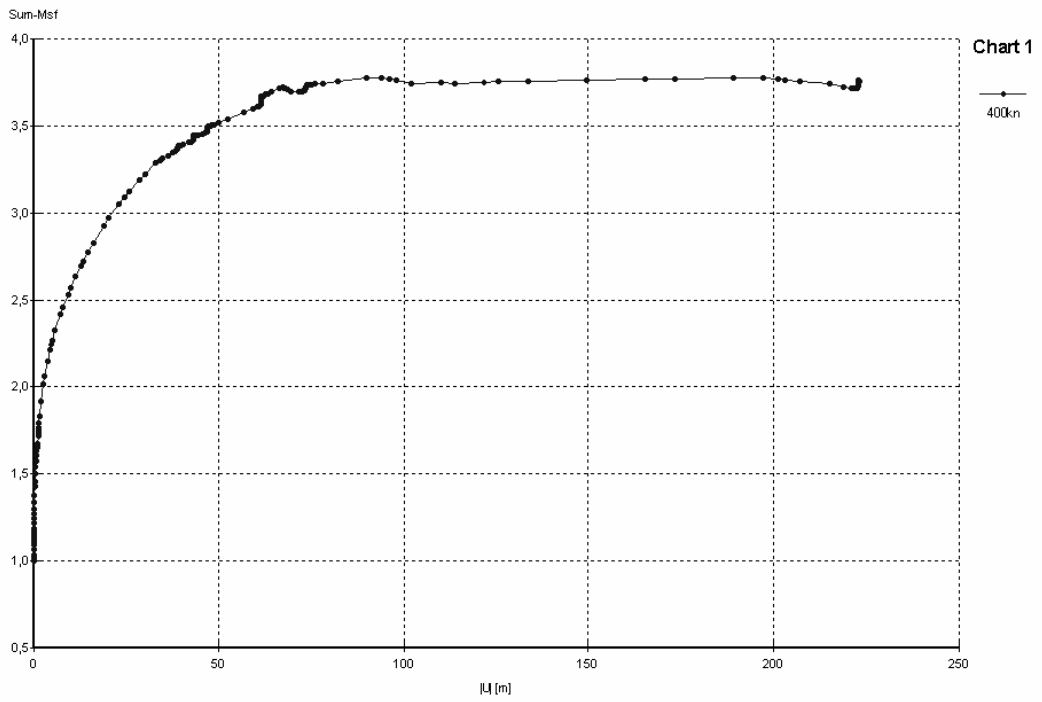


Figure A.11. Factor of safety with 400 kN ring load,  $\phi=35^{\circ}$ ,  $R_{\text{interface}}=0.5$

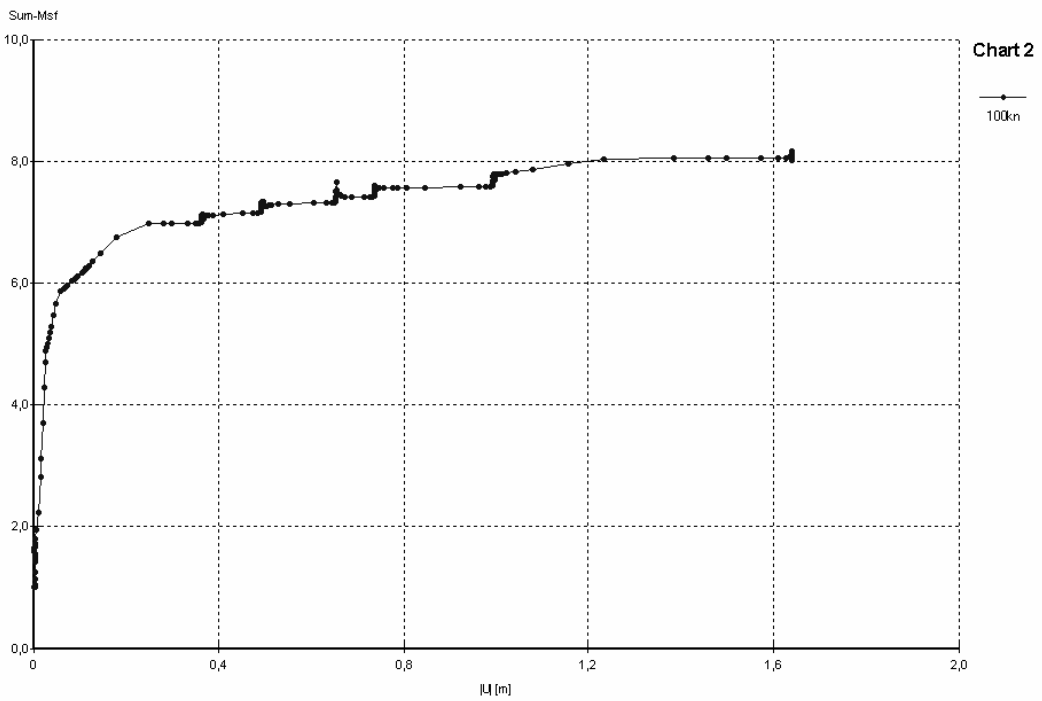


Figure A.12. Factor of safety with 100 kN ring Load,  $\phi=31^{\circ}$ ,  $R_{\text{interface}}=0.75$

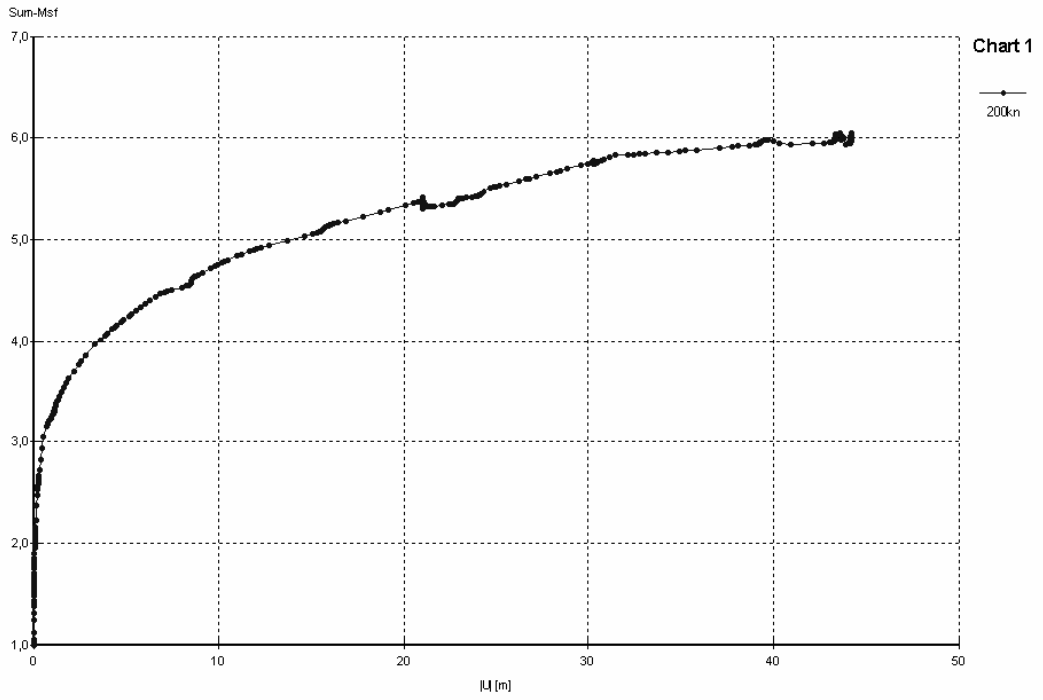


Figure A.13. Factor of safety with 200 kN ring load,  $\varphi=31^0$ ,  $R_{interface}=0.75$

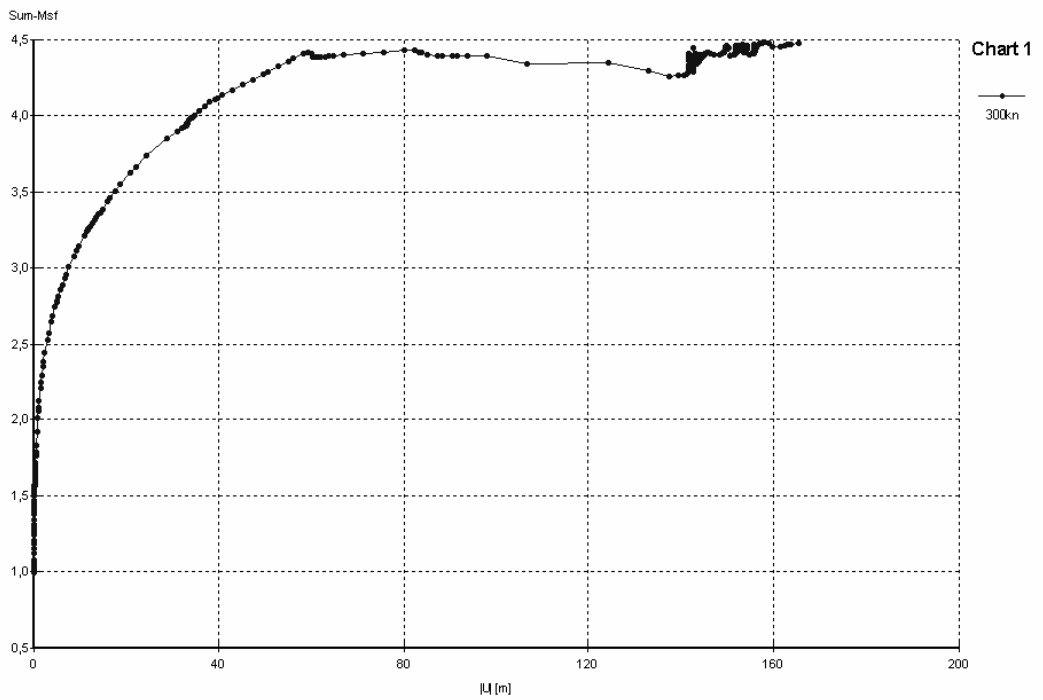


Figure A.14. Factor of safety with 300 kN ring load,  $\varphi=31^0$ ,  $R_{interface}=0.75$

The system collapsed when 400 kN load was applied. So there is no result of 400 kN with  $\varphi=31^0$  and 0.75 value of interface.

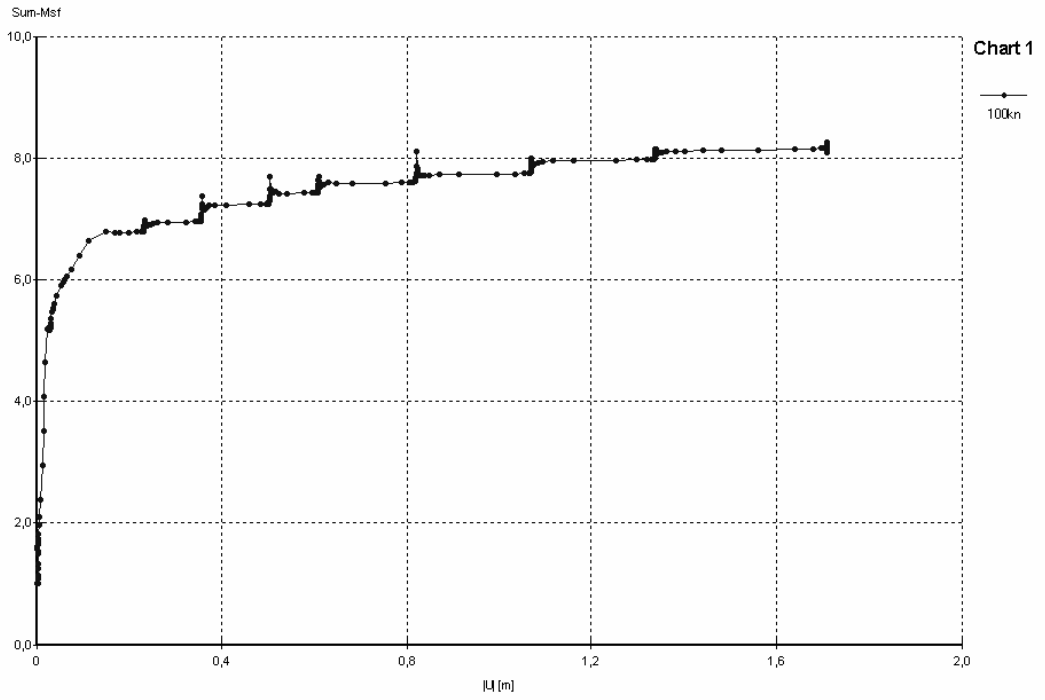


Figure A.15. Factor of safety with 100kN ring load,  $\varphi=33^0$ ,  $R_{interface}=0.75$

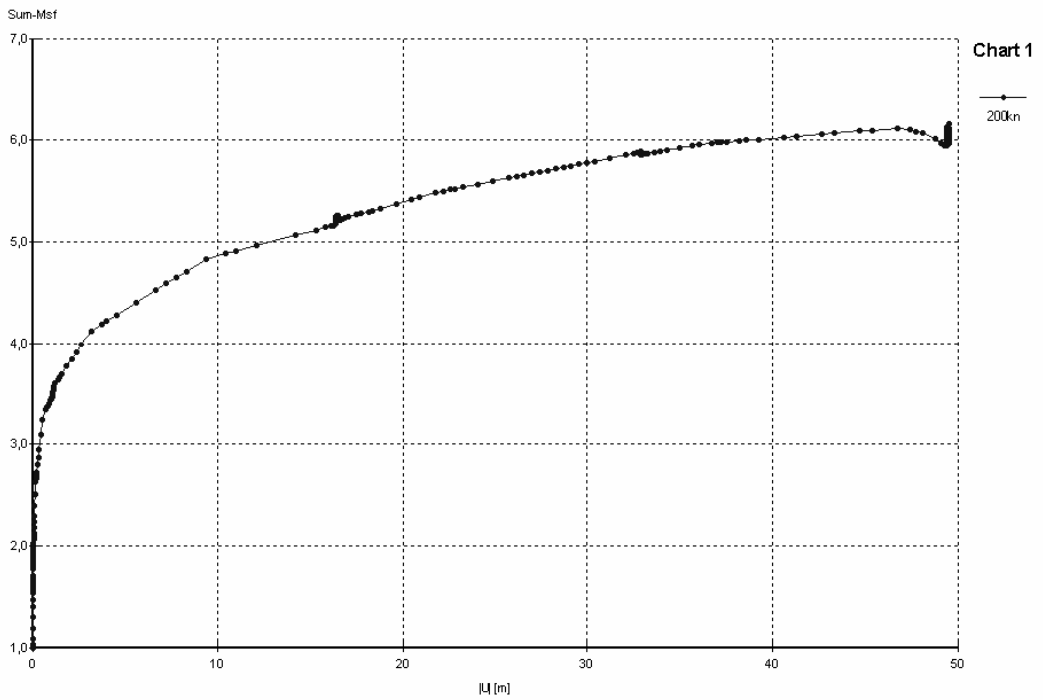


Figure A.16. Factor of safety with 200kN ring load,  $\varphi=33^0$ ,  $R_{interface}=0.75$

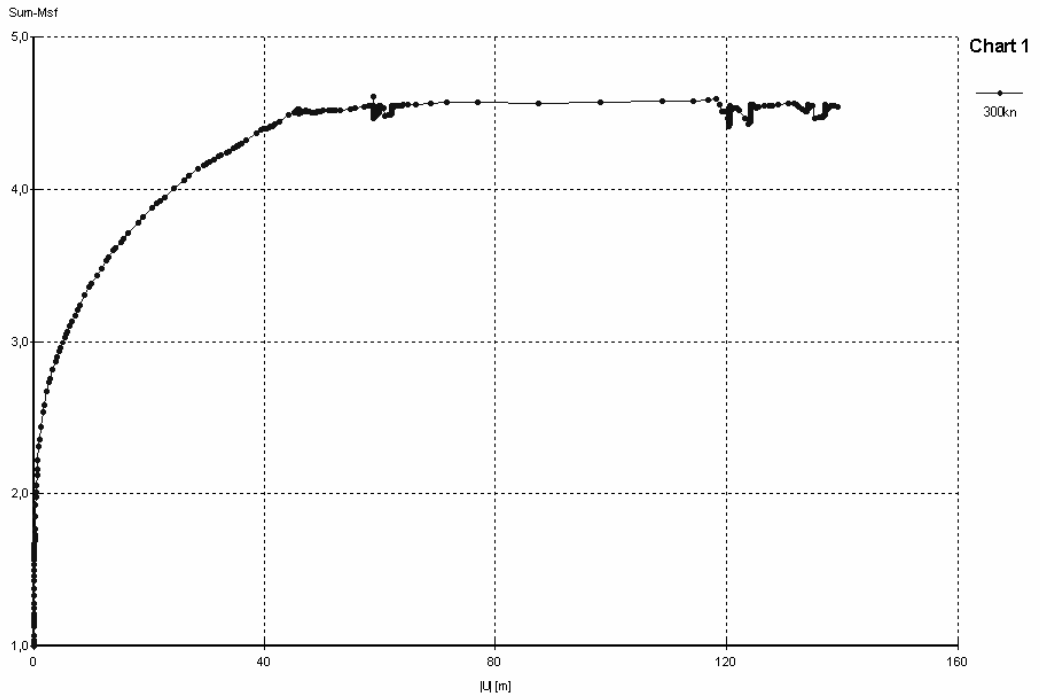


Figure A.17. Factor of safety with 300kN ring load,  $\varphi=33^{\circ}$ ,  $R_{\text{interface}}=0.75$

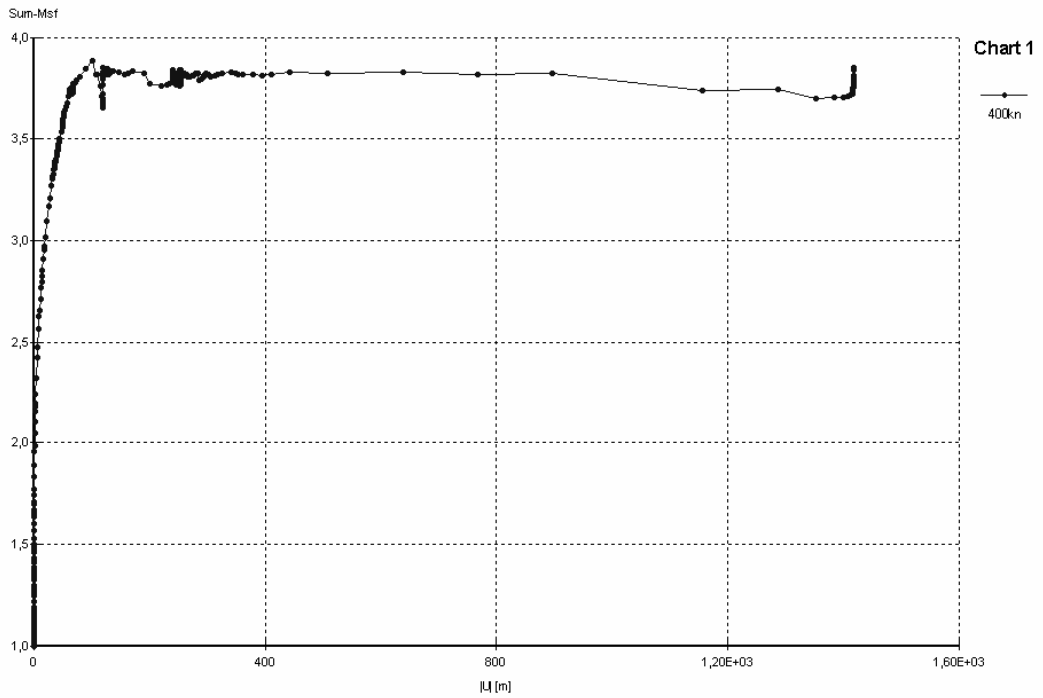


Figure A.18. Factor of safety with 400kN ring load,  $\varphi=33^{\circ}$ ,  $R_{\text{interface}}=0.75$

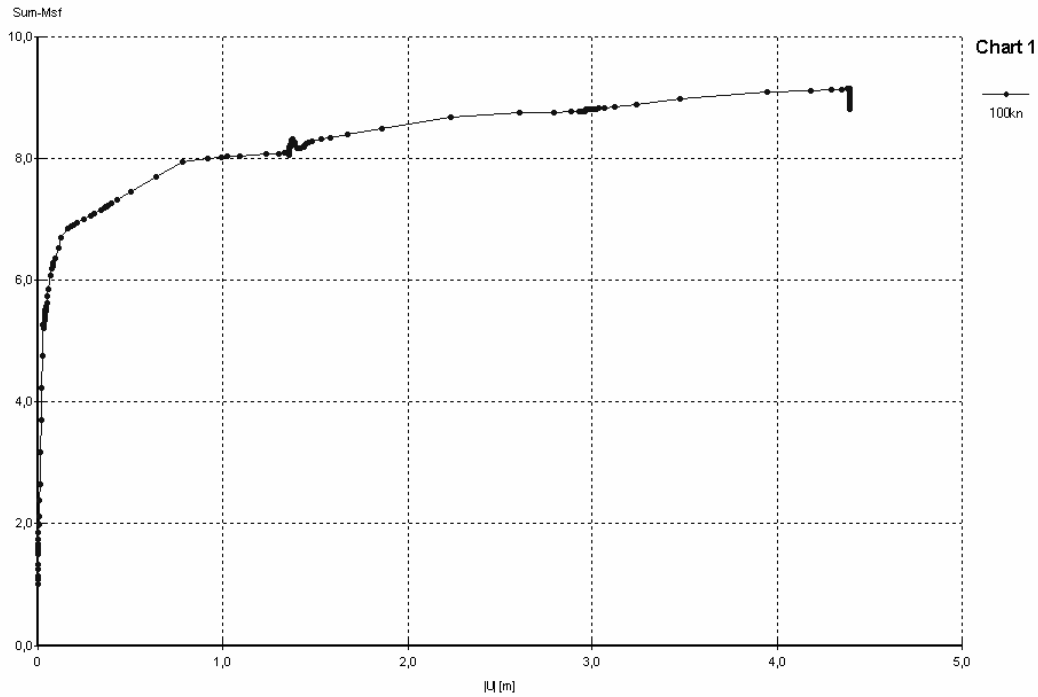


Figure A.19. Factor of safety with 100kN ring load,  $\varphi=35^0$ ,  $R_{interface}=0.75$

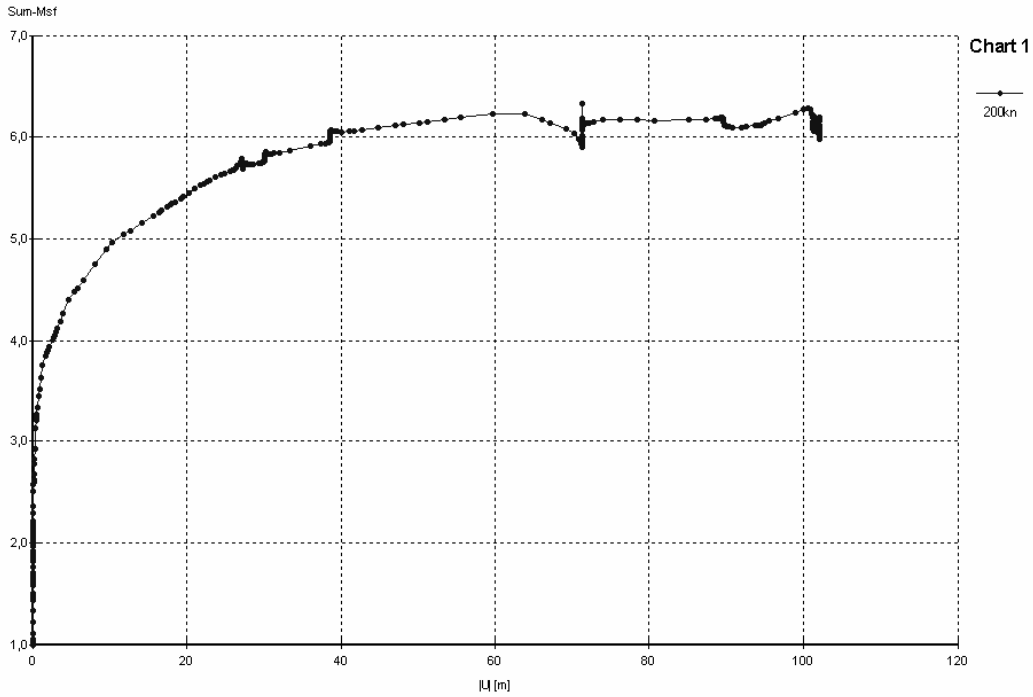


Figure A.20. Factor of safety with 200kN ring load,  $\varphi=35^0$ ,  $R_{interface}=0.75$

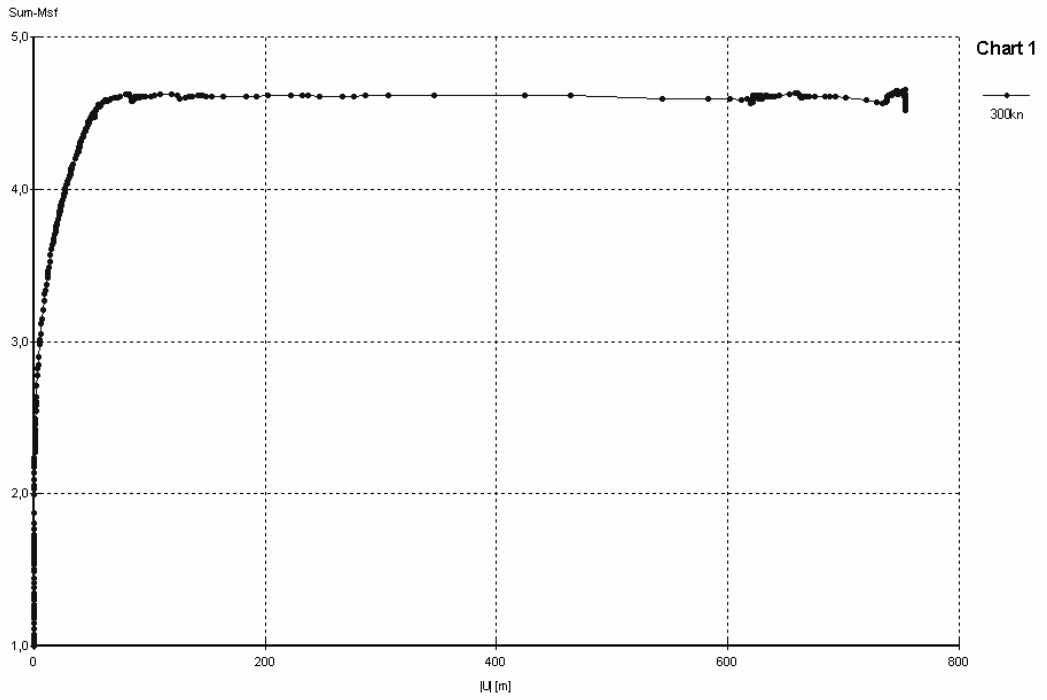


Figure A.21. Factor of safety with 300 kN ring load,  $\phi=35^0$ ,  $R_{\text{interface}}=0.75$

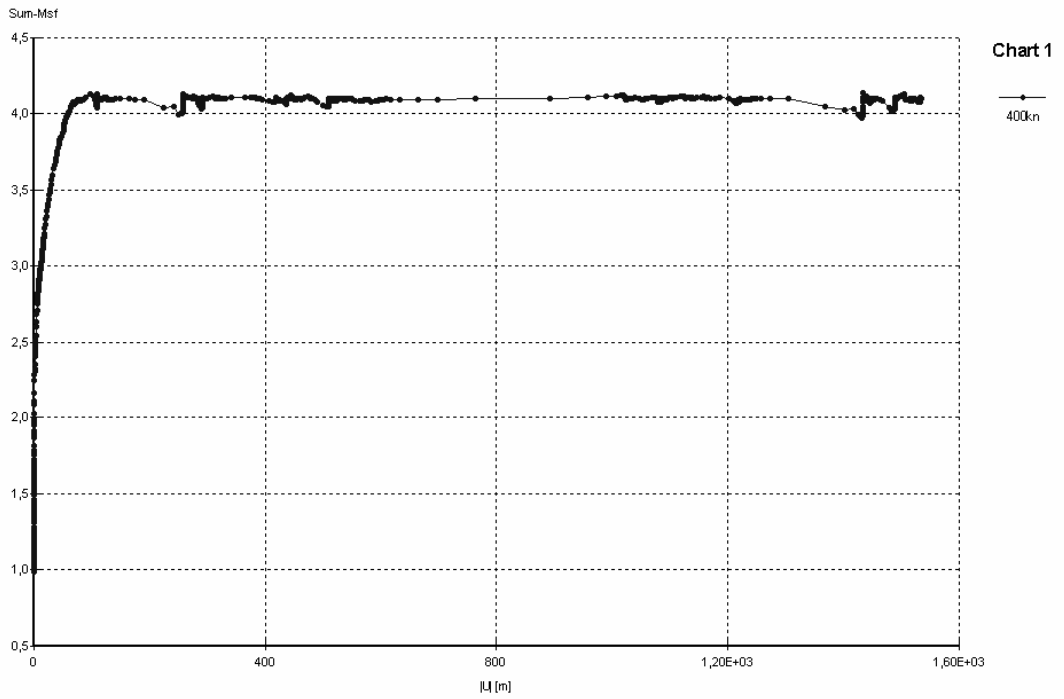


Figure A.22. Factor of safety with 400 kN ring load,  $\phi=35^0$ ,  $R_{\text{interface}}=0.75$

## REFERENCES

- Bowles, J. E., 1988, *Foundation Analysis and Design, Fourth Edition*, McGraw-Hill, Singapore.
- Broms, B.B., 1966, *Methods of Calculating the Ultimate Bearing Capacity of Piles - A Summary*, Sols-Sols No. 18-19, 21-32.
- Er, Berrak, 1998, *Ultimate Bearing Capacity of Piles Under Load Tests*, M.S. Thesis, Boğazici University, Institute for Graduate Studies in Science and Engineering.
- International Course on Computational Geotechnics, 1-3 September 2002, Istanbul Technical University.
- Meyerhof, G. G., 1976, "Bearing Capacity and Settlement of Pile Foundations", *J. Geotech. Eng. Div. ASCE*, Vol. 102, No. GT3, pp. 197-228.
- Department of the Navy, 1988, "Foundations and Earth Structures", *NAVFAC Design Manuals 7.1 and 7.2*, Alexandria, VA.
- PCI, 1993, *Precast/Prestressed Concrete Institute Journal*, Volume 38, No. 2, March-April.
- PLAXIS manuals and website, 2007,  
<http://www.plaxis.nl/index.php?cat=manuals&mouse=Plaxis%20V8>
- Portland Cement Association [PCA], 1951, *Concrete Piles: Design, Manufacture and Driving*.
- U.S. Department of Transportation, 1998, *Design and Construction of Driven Pile Foundations*.

Yıldırım, Sönmez, 2002, *Zemin İncelemesi ve Temel Tasarımı*, Birsen Yayınevi, İstanbul.

## REFERENCES NOT CITED

Braja, M. Das, 2004, *Principles of Foundation Engineering*. Pacific Grove, CA: Thomson/ Brooks/ Cole.

Coduto, Donald P., 2001, *Foundation Design Principles and Practices*, Pearson Prentice-Hall, New Jersey.